Journal of Medicinal Chemistry

Perspective

pubs.acs.org/jmc

Small Molecules That Target Protein Misfolding

Lori Krim Gavrin, Rajiah Aldrin Denny, and Eddine Saiah*

BioTherapeutics Chemistry, Pfizer Worldwide Medicinal Chemistry, 200 CambridgePark Drive, Cambridge, Massachusetts 02140, United States

ABSTRACT: Protein misfolding is a process in which proteins are unable to attain or maintain their biologically active conformation. Factors contributing to protein misfolding include missense mutations and intracellular factors such as pH changes, oxidative stress, or metal ions. Protein misfolding is linked to a large number of diseases such as cystic fibrosis, Alzheimer's disease, Parkinson's disease, amyotrophic lateral sclerosis, and less familiar diseases such as Gaucher's disease, nephrogenic diabetes insipidus, and Creutzfeldt−Jakob disease. In this Perspective, we report on small molecules that bind to and stabilize the aberrant protein, thereby helping it to attain a native or near-native conformation and restoring its function. The following targets will be specifically discussed: transthyretin, p53, superoxide dismutase 1, lysozyme, serum amyloid A, prions, vasopressin receptor 2, and α-1-antitrypsin.

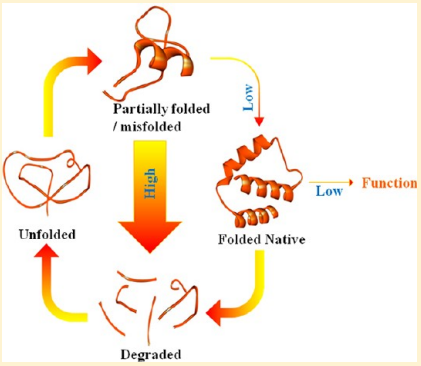

INTRODUCTION

In order for a protein to be functional, it needs to be correctly folded into its tertiary structure. Almost all proteins that contain an amino acid mutation or mutations have a tendency to improperly fold, i.e., misfold. However, mutations are not the only culprit leading to protein misfolding, as more than 30 known wild type proteins also have an intrinsic propensity to misfold. Intracellular factors such as pH, oxidative stress, and metal ions can also play a critical role in protein misfolding. Protein misfolding is currently linked to more than 25 diseases,[1] including well-known diseases such as cystic fibrosis, Alzheimer's disease, Parkinson's disease, and ALS (amyotrophic lateral sclerosis or Lou Gehrig's disease), as well as less familiar diseases such as Gaucher's disease, nephrogenic diabetes insipidus, and Creutzfeldt−Jakob disease. Protein misfolding diseases are becoming increasingly more common as the population ages. This is due to a variety of factors including mutations, thermodynamics, and external stress factors, all contributing to a significant increase in the number of protein misfolding incidences.

The diseases caused by protein misfolding are believed to occur via a loss or gain of protein function (Figure 1).[2] For instance, loss of function (LOF) occurs if the misfolding results in the inability of the protein to achieve its functional conformation. Alternatively, a LOF disease can occur if the misfolded protein cannot reach its required site of action in the cell. For instance, if the misfolded protein is not recognized by transport proteins and is unable to traffic to its functional location within the cell, it will not be able to exert its biological function. The loss of function diseases are generally caused by inherited or somatic mutations and include cystic fibrosis, lysosomal storage diseases such as Gaucher disease, α1-antitrypsin deficiency, and certain cancers. On the other hand, gain of function (GOF) toxicity is often caused by the aggregation (amyloids or fibrils) of a misfolded protein that can adversely affect cell function. Proteins mutated in GOF diseases turn on cellular processes that normally do not occur in a healthy cell, thus triggering disease pathology.[3] Several subsets of neurodegenerative diseases such as Alzheimer's disease, Parkinson's disease, ALS, and a wide range of amyloidoses can be categorized as GOF diseases. The gain of function diseases are often age-related and are caused by the accumulation of amyloid or amyloid-like aggregates of the pathogenic protein.

Folding in the cell occurs in a highly crowded environment containing 200−300 mg/mL protein.[4] The cellular machinery has evolved to assist and control proper protein folding, trafficking, and turnover. Cells have developed a diverse set of molecular chaperones that interact and stabilize nonfolded proteins to reach their native conformation.[5] Chaperones typically recognize the exposed hydrophobic side chains of non-native conformations and shield these features from the solvent, thus suppressing aggregation and promoting folding. Many of these natural chaperones are heat shock proteins (Hsps) whose synthesis is up-regulated under conditions of stress, elevated temperatures, or oxidative conditions.[6] Down-regulation of chaperone activity can result in the accumulation of misfolded proteins that may lead to aggregation and cell toxicity.[7]

The molecular chaperones, proteases, and accessory factors that work together to refold or remove proteins are known collectively as protein quality control systems. Protein quality control systems consist of two parts: one that supervises and supports folding/refolding and protects folding intermediates from aggregation and one that eliminates proteins with a decreased or abolished capacity to fold to the native state. The protein quality control system responsible for the maintenance of protein structure and function is also known as protein homeostasis (i.e., proteostasis). Both LOF and GOF protein

Received: August 10, 2012
Published: October 17, 2012

dx.doi.org/10.1021/jm301182j | J. Med. Chem. 2012, 55, 10823−10843

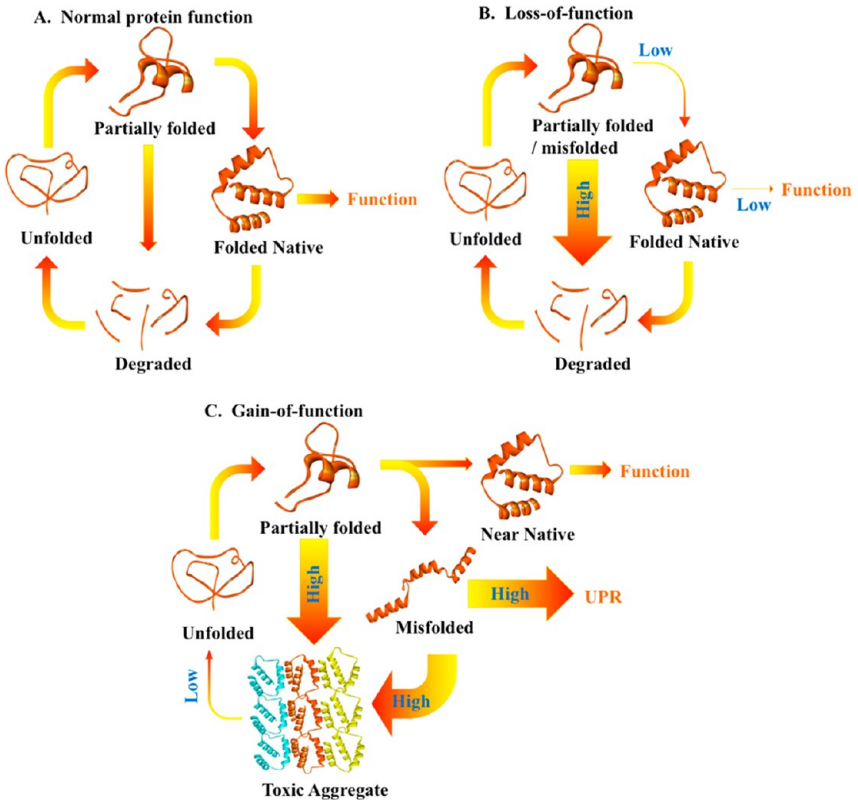

Figure 1. (A) Schematic representation of normal protein function. The translated protein sequence in the endoplasmic reticulum (ER) in the unfolded state under protein homeostasis condition folds to its native form via intermediate partially folded state(s). The folded native protein migrates to the site of action and performs its normal function. After fulfilling its functional role, the protein is degraded to individual amino acids by various proteases in the lysosomes. (B) Loss of function arises from the inability of a misfolded protein to perform a necessary function because of a failure to fold to the native conformation or high clearance of the partially folded or misfolded protein. (C) Gain of function arises because of toxic protein aggregates and/or hyperactivation of signaling pathways by unfolded protein response (UPR).

misfolding diseases could be remedied through this route. Examples of proteostasis modulators are HSF1 activators, HSP inducers and inhibitors, ubiquitin targeted proteins, and proteosome inhibitors.

Protein misfolding covers a wide range of diseases and biological pathways and cannot be covered in a single Perspective because of space constraints. Therefore, we decided to focus our attention on small molecules that directly target proteins that undergo misfolding and aggregation. Protein misfolding topics not covered in this Perspective because of space constraints or because of recently published reviews include (1) mechanisms and strategies related to post-translational modifications that modulate protein misfolding and aggregation, (2) proteostasis pathways that modulate protein misfolding and aggregation,[6,7] (3) cystic fibrosis,[8] lysosomal storage diseases,[9] and Alzheimer's disease,[10] (4) small molecules that prevent aggregation in GOF diseases or restore function in LOF diseases without a clear mechanism of action.[11]

We are reporting below on small molecules that restore a native or seminative conformation and function by binding to and thereby stabilizing the misfolded protein. Specifically, this paper will describe compound modulation of the following proteins: transthyretin, p53, superoxide dismutase 1, lysozyme, serum amyloid A, prions, vasopressin receptor 2, and α-1-antitrypsin, all of which are prone to misfolding. We included examples of small molecules that alter protein misfolding as well as structural and biophysical information about the binding modes of these molecules. We hope that the reader will learn more about this exciting area of research. Additionally, we aim to demonstrate to the medicinal chemistry community that small molecule modulation of protein misfolding not only is possible but also offers innovative opportunities for drug discovery.

TRANSTHYRETIN (TTR)

Transthyretin (TTR) is a 55 kDa homotetrameric protein in which each of the 4 identical subunits comprises 127 amino acids. TTR is synthesized in the liver and the choroid plexus of the brain and is then secreted into the blood or cerebrospinal fluid (CSF). TTR has two thyroxine, or T4 (**1**, Figure 2), binding sites within each tetramer and is the primary transporter of thyroxine in the CSF. However, TTR rarely

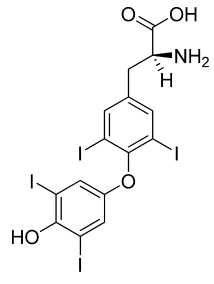

Thyroxine (1)

Figure 2. Structure of thyroxine (T4), **1**.

dx.doi.org/10.1021/jm301182j | J. Med. Chem. 2012, 55, 10823−10843

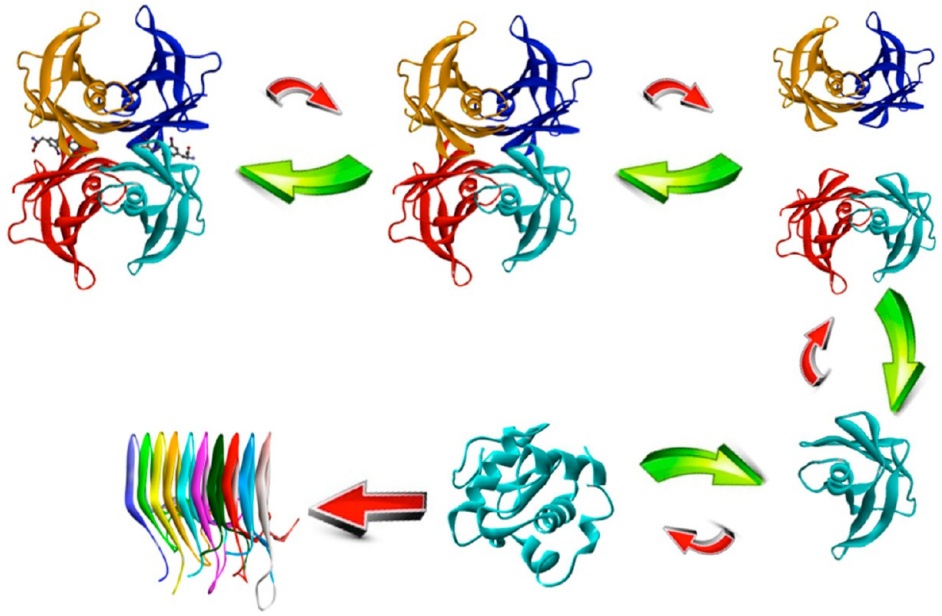

Figure 3. Representation of the transthyretin amyloid formation cascade. TTR amyloid formation requires slow tetramer dissociation (top center) to a pair of dimers (top right), which then quickly dissociate to form folded monomers (bottom right). Monomer conformational change (bottom center) results in an aggregation-prone amyloidogenic intermediate. The amyloidogenic intermediate can misassemble to form a variety of aggregate morphologies, including spherical oligomers, amorphous aggregates, and fibrils (bottom left).

transports thyroxine in the blood, leaving >99% of the thyroxine binding sites unoccupied.[12,13] In the blood, the major carriers of T4 are thyroid-binding globulin (TBG) and albumin. The main role of peripheral TTR is transporting retinol (vitamin A) through its association with retinol binding protein (RBP). The thyroxine and RBP binding sites do not overlap,[14] and there is no evidence that occupancy of the RBP sites influences the affinity for thyroxine binding of TTR.[15]

TTR protein can cause a GOF disease, as it can misfold and consequently form amyloid fibrils in humans.[16,17] There are many known single point mutations that initiate TTR misfolding/aggregation. However, it is important to note that WT TTR itself is also amyloidogenic. TTR amyloid fibrils deposit in a variety of organs including the nerves, heart, and kidneys, thus interfering with normal organ function. Wild type TTR aggregation causes senile systemic amyloidosis (SSA), a cardiomyopathy that affects up to 20% of the population over age 65.[18,19] Variant TTR deposition leads to familial amyloid cardiomyopathy (FAC) for those with the V122I-TTR mutation,[20,21] familial amyloid polyneuropathy (FAP) for those with the V30M-TTR mutation,[22] and central nervous system amyloidoses (CNSA) for people having the D18G and A25T mutations.[23,24] There are also over 100 other known single point mutations of TTR that lead to FAP.[25,26]

There is great variation in TTR-FAP severity and age of onset, though the factors that influence these variations are unknown.[27] It is estimated that there are 5000−10 000 patients worldwide with TTR-FAP.[28] The disease is characterized by progressive sensory, motor and autonomic impairment, which typically leads to death around a decade after diagnosis, often due to cachexia.[27] Although the exact number of V122I-associated cases of FAC is unknown, it is estimated that there are ∼100 000 to 150 000 symptomatic patients above the age of 65 in the U.S. alone.[21,29] Until recently, the only available treatment for FAP was liver transplantation to replace the mutant TTR secreting liver with a WT-TTR secreting liver.

The TTR misfolding to aggregation pathway has been studied in great depth.[30] From this work, it was discovered that TTR tetramer dissociation is the rate-limiting step in the amyloid formation cascade. Tetramer dissociation is followed by dimer dissociation yielding unstable TTR monomers. The TTR monomers easily unfold leading to spontaneous self-assembly into TTR amyloid fibrils,[31] as depicted in Figure 3.

As shown in Figure 3, the natural TTR ligand thyroxine binds at pockets formed by the interfaces of the two dimers. It was hypothesized that the binding of thyroxine, or a mimetic, would stabilize the dimer−dimer interface, thereby reducing tetramer dissociation and preventing fibril formation. A small molecule "kinetic stabilizer" should stabilize the tetramer over the dissociated dimers by selectively binding to the tetramer. In turn, this binding increases the free energy of activation required for dissociation by lowering the energy of the tetramer, slowing the conversion rate of starting material (tetramer) to product (amyloid).[32] In a proof of concept study, it was shown that both thryoxine and its analogue 2,4,6-triiodophenol (**2**,[33] Figure 4) inhibited TTR amyloid formation, supporting the kinetic stabilizer hypothesis.[33]

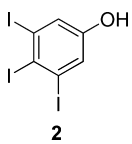

2

Figure 4. Structure of **2**, the first ligand to show reduction in TTR amyloid formation by stabilization of TTR tetramer.

There have been vigorous screening efforts and structure based drug design (SBDD) programs to identify small molecule stabilizers of the TTR tetramer. Over 1000 aromatic small molecules have been designed and synthesized that kinetically stabilize the TTR tetramer.[34] The majority of these compounds were designed by taking advantage of the thyroxine-TTR

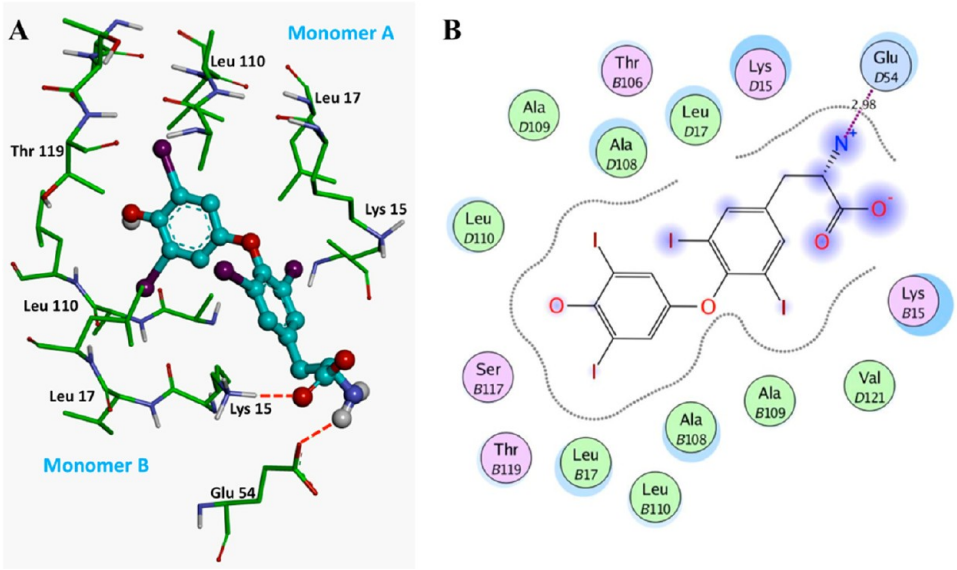

Figure 5. One possible binding interaction of thyroxine with the WT-TTR between two monomers A and B is illustrated. Panel A shows one representation of the 3D interaction of thyroxine (ball and stick) at the dimer interface and the TTR side chains (wire). Hydrogen bond interactions between the Glu54 and Lys15 with the amide and the acid groups in thyroxine, respectively, are highlighted by red dashed dots. Monomer A and B carbon atoms are represented in green. Panel B provides a 2D interaction diagram of thyroxine with TTR. The structure of the complex was generated from its X-ray coordinates (PDB code 2ROX) and was produced using Discovery Studio.[49]

structural information, as shown in Figure 5A. In order to mimic thyroxine, binders in this pocket typically have two differentially substituted aromatic rings connected by a variety of linkers. One aryl ring has polar substituents enabling electrostatic interactions, while the other aryl group tends to have halogen or alkyl substituents that complement the hydrophobic halogen binding pockets (HBPs) in the inner or outer cavity of the thyroxine binding site, as shown in Figure 5B. It is not surprising that thyroxine mimetics have a bis-aryl motif resembling the natural ligand. However, the vast degree of structural diversity that is tolerated in the aryl linking region is remarkable. Molecules with a wide variety of linker lengths, bond types, and heteroatoms maintain affinity in this region.[32]

Interestingly, most compounds binding in the thyroxine pockets of TTR bind with negative cooperativity, meaning that the first molecule binds more tightly than does the second molecule to the tetramer. Furthermore, it has been demonstrated that binding to a single thyroxine binding site imparts enough stability to the TTR tetramer to reduce dissociation.[35] In addition to potency, compound selectivity to the thyroxine binding site on TTR is critical so as not to disrupt its normal binding to and transport by albumin.[36]

The TTR kinetic stabilizer work has culminated in the advancement of two compounds into clinical trials. Diflunisal[37] (**3**, Figure 6) is an FDA approved non-steroid anti-inflammatory drug (NSAID) that has high structural similarity to thyroxine. Acting as a thyroxine mimic, diflunisal was found to bind to TTR with negative cooperativity (K_{d1} = 75 nM; K_{d2} = 100 nM)[38] and is currently in phase III to test its efficacy in the treatment of FAP, FAC, and SSA. However, diflunisal shows only modest selectivity for TTR over other plasma proteins. Diflunisal is being dosed at 250 mg b.i.d. in patients in the TTR amyloidosis trials. The second TTR kinetic stabilizer, tafamidis[39] (**4**, Figure 6), was discovered at Scripps[40] and was developed by FoldRx (acquired by Pfizer). Tafamadis (trade name Vyndaqel) also binds to TTR with negative cooperativity (K_{d1} = 2 nM; K_{d2} = 200 nM) and shows excellent selectivity for

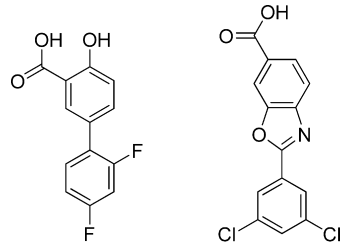

Diflunisal (3) **Tafamidis (4)**

Figure 6. Clinical candidates for the treatment of TTR amyloidosis.

TTR over other plasma proteins.[36] Tafamidis meglumine was recently approved by the European Commission for the treatment of TTR-FAP[41] in adult patients with stage 1 symptomatic familial polyneuropathy. Tafamidis is the first disease modifying pharmacological treatment available to treat TTR-FAP.

Recently, covalent small molecule stabilizers such as **5**[42] (Figure 7) that bind to the thyroxine binding site of the TTR tetramer were disclosed.[42] Compound **5** was shown to react chemoselectively with Lys-15, one of eight lysine amino groups in TTR. The binding site of these molecules was confirmed unambiguously by the use of X-ray crystallography. This class of

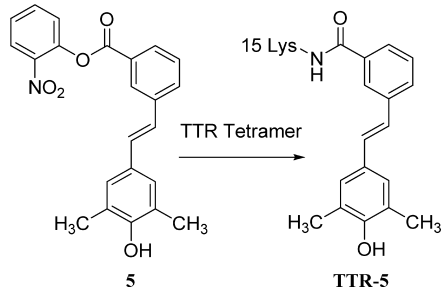

5 **TTR-5**

Figure 7. Structure of covalent kinetic stabilizer **5**.

dx.doi.org/10.1021/jm301182j | J. Med. Chem. 2012, 55, 10823−10843

compounds was found to reduce TTR amyloid fibril formation in vitro by a greater amount than the corresponding noncovalent analogues. It is possible that taking advantage of the chemoselective reactivity of the active site lysine could provide an alternative strategy for the treatment of TTR amyloidosis using covalent small molecule kinetic stabilizers.

Another new and promising approach to treat TTR amyloidosis is with the use of bivalent kinetic stabilizers. A bivalent kinetic stabilizer is a molecule that binds to both of the T4 binding sites in the TTR tetramer at the same time. Kolstoe and co-workers have designed and synthesized palindromic ligands such as **6**[43] (Figure 8A) that bind with high affinity to

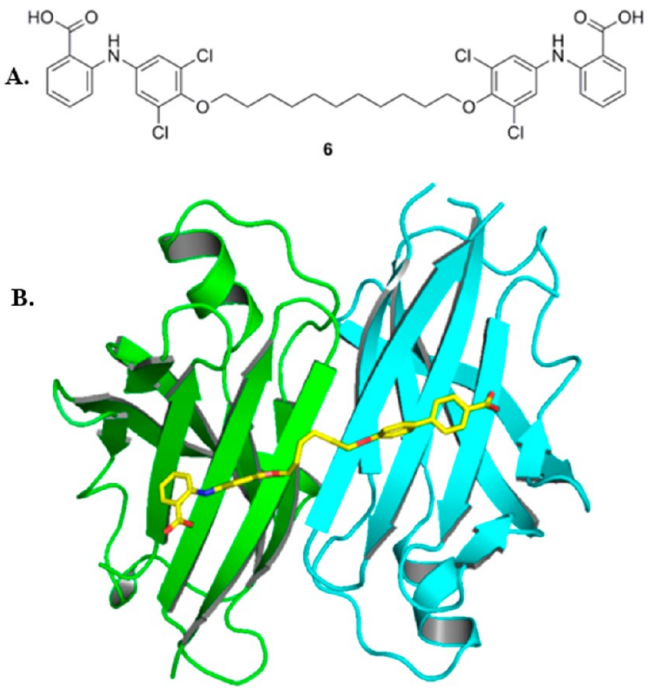

Figure 8. (A) Structure of **6**, a bivalent kinetic stabilizer. (B) Cocrystal structure of palindromic ligand, **6**, with TTR. Only the TTR dimer of the tetramer is shown. Monomers are colored in green and cyan, and the carbon atoms of **6** are shown in yellow. 2FLM PDB coordinates were used to generate the figure using the PyMOL software package.[45]

TTR tetramers under physiological conditions.[43] A cocrystal structure of the bivalent stabilizer **6** with TTR (Figure 8B) confirmed the original proposal by Green[44] who suggested that two biaryl ligands linked by a 7−10 Å alkyl chain would fit comfortably into both thyroxine binding sites on TTR. A few of the bivalent analogues have demonstrated bioavailability (F = 12% in mice when dosed at 5 mpk po) and could represent a new avenue of exploration for the treatment of TTR amyloidoses.

p53

The tumor suppressor protein p53 is a transcription factor that has an essential role in guarding the cell in response to various stress signals through the induction of cell cycle arrest and apoptosis as well as effects that are independent of its ability to transactivate gene expression.[46] Mutation of the tumor suppressor p53 is the most frequent genetic alteration in human cancer. p53 inactivation in tumors occurs through two general mechanisms: inactivation by point mutations in p53 itself or through the inactivation of signaling pathways that regulate p53 activity. Most p53 mutations are missense mutations and cause single amino acid changes at many different positions. These mutations are diverse in their type, sequence context, position, and structural impact.[47]

p53 is biologically active as a homotetramer comprising 4 units containing 393 amino acid residues each. The p53 structure contains an amino terminal transactivation domain (TAD), a proline-rich region (PRR), a folded DNA-binding domain (DBD), and tetramerization domains connected with a flexible linker region (Figure 9). The majority of the mutations

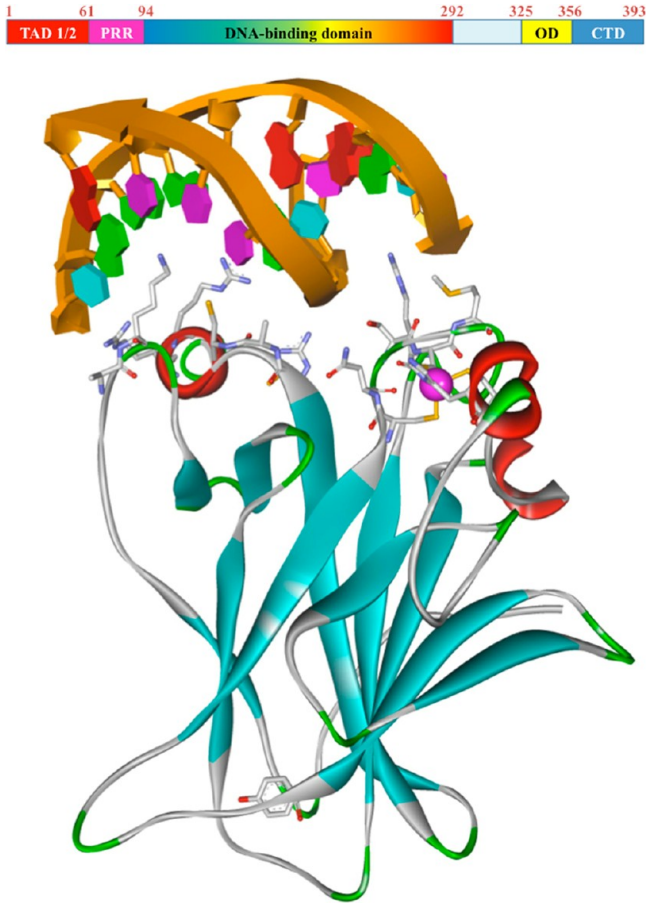

Figure 9. Structural schematic of p53 interaction with DNA. 1TUP PDB coordinates were used to generate this structure. Zinc is represented in magenta CPK. The DNA double helix backbone is represented as a light brown arrow, and base pair side chains are shown as different colored rings. p53 is shown as a solid ribbon. p53 residues that interact with the DNA and bind the zinc are shown as stick representation. Helices are shown in red, sheets in cyan, loops in white, turns in green. The Tyr220 mutation in the crystal structure is shown in stick representation. The picture was generated using Discovery Studio, version 3.1.[49]

occur in the DNA-binding domain of the p53 protein (residues 102−292), and they result in loss of DNA binding. The crystal structure of a complex containing the core domain of human p53 and a DNA binding site has been determined at 2.2 Å resolution. The core domain structure consists of a β sandwich that serves as a scaffold for two large loops and a loop−sheet−helix motif. The two loops, which are held together in part by a tetrahedrally coordinated zinc atom, and the loop−sheet−helix motif form the DNA binding surface of p53.

dx.doi.org/10.1021/jm301182j | J. Med. Chem. 2012, 55, 10823−10843

Zinc binding (coordinated by His179, Cys176, Cys238, and Cys242) is critical for correct folding and requires reduction of thiol groups on cysteines. Residues from the loop−sheet−helix motif interact in the major groove of the DNA, while an arginine from one of the two large loops interacts in the minor groove. The loops and the loop−sheet−helix motif consist of the conserved regions of the core domain and contain the majority of the p53 mutations identified in tumors.[48]

Types of p53 Mutants. p53 mutant proteins are classified as contact mutants or structural mutants. DNA-contact mutants retain the overall architecture of the DBD with loss of a critical DNA contact. They may actively prevent DNA binding if a large hydrophobic side chain is introduced. Examples of such mutations include S241F, R248W, and C277F. Zinc-binding mutants affect the zinc coordination sphere. Examples include C176F, H179R, and C242F. This category includes R175H, the most frequent hotspot mutant, because introduction of histidine causes distortions that directly interfere with zinc binding. Structural mutants cause distortions that create internal cavities or surface crevices in the protein scaffold, inducing conformational changes in the DNA binding surface. This highlights the structural heterogeneity of mutant proteins, with consequences for their biochemical and biological properties.[3]

Destabilized mutants of p53 can be stabilized by the binding of other molecules. This has been shown by the binding of a specific double-stranded DNA,[50] heparin,[51] or a synthetic peptide.[52] Those molecules bind to the wild-type p53 core domain and should bind generically to most mutants. Other molecules have been proposed to stabilize the folded state of the core domain of p53 such as CP-31398[53] and will be discussed below.

Small Molecules That Stabilize and Reactivate Mutant p53. Screening approaches and rational drug design have led to the identification of mutant p53-targeting compounds with different structures and properties. We focus in this section on compounds that were shown to bind and stabilize mutant p53. One of the first small molecules identified to reactivate p53 was compound **7** (CP-31398).[53] Upon screening of a library of over 100 000 compounds and further optimizing of the hits, compound **7** was shown to promote the conformational stability of wild-type p53 DBD and that of full-length p53. However, follow-up studies suggest that the molecule does not directly bind to p53 but intercalates with DNA and destabilizes the DNA-p53 core domain complex.[51]

Screening of the diversity set from the National Cancer Institute led to the discovery of two small molecules with mutant p53-reactivating capacity: compound **8**[54] known as PRIMA-1 (p53 reactivation and induction of massive apoptosis) and compound **9**[54] known as MIRA-3 (mutant p53 dependent induction of rapid apoptosis), as shown in Figure 11. Additional screening of small compound libraries also identified compound **10**[55] (Figure 10) known as STIMA-1 (SH group-targeting compound that induces massive apoptosis), Figure 11.

The exact mechanism by which compound **8** stabilizes mutant p53 is not clear; however, compounds **9** and **10** share the ability to alkylate thiol groups. Zache et al.[56] proposed that alkylation of one or several of the 10 cysteine residues in the p53 core domain may be responsible for the mutant p53-dependent effect of these compounds.

Fersht et al.[57] solved high-resolution crystal structures of several p53 oncogenic mutants to investigate the structural

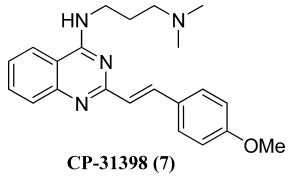

CP-31398 (7)

Figure 10. Structure of quinazoline **7**.

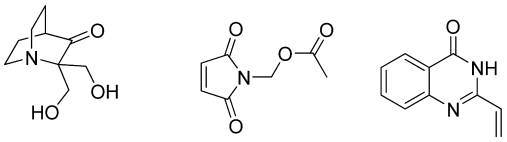

PRIMA-1 (8) MIRA-3 (9) STIMA-1 (10)

Figure 11. Structures of small molecules, **8**, **9**, and **10**, reported as p53 reactivators.

basis of inactivation and provide information for designing drugs that may rescue inactivated mutants. They found a variety of structural consequences upon mutation including the creation of large, water-accessible crevices or hydrophobic internal pockets with a large loss of thermodynamic stability, suggesting that some mutants have the potential of being rescued by a stabilizing drug. Following up on this finding, Fersht et al.[58] performed an in silico analysis of the crystal structure of the Y220C mutant using virtual screening and rational drug design. Compounds were screened for binding to p53 using NMR spectroscopy. Compound **11**[58] (Figure 12)

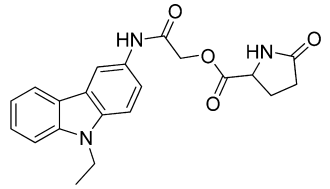

11

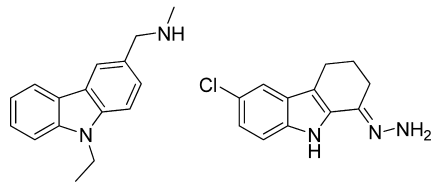

12 13

Figure 12. Small molecules binders of Y220C-p53 mutant.

was shown to bind to the mutation-induced cleft of p53C-Y220C mutant with a K_d of 213 μM but did not bind to the wild type. Additional screening led to the identification of compound **12**[58] (Figure 12) with a binding K_d of 140 μM. This compound stabilizes the Cys220 mutant in a concentration-dependent manner, raising the melting temperature by almost 2 °C and increasing the half-life from 3.8 to 15.7 min.

Fersht et al. also described the use of fragment screening and molecular dynamics (MD) simulations to further explore the druggable surface of the p53-Y220C mutant.[59] The authors attempted to identify all possible ligand interaction sites (i.e., "hot spots") on the surface of the mutational cavity, which collectively provide a blueprint for the design of molecules that bind to p53-Y220C with good affinity (Figure 13). Compound **13**[59] (Figure 12) was shown to have the tightest binding affinity

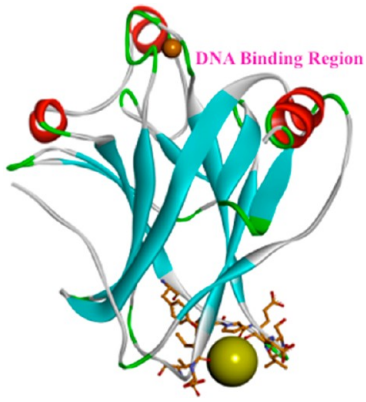

Figure 13. Binding site of carbazole derivatives in p53 pocket shown in yellow sphere. Residues lining this binding site are shown as brown sticks. The zinc atom is shown in brown CPK representation. Helices are shown in red, sheets in cyan, loops in white, turns in green. The picture was generated using Discovery Studio, version 3.1.[49]

with a K_d = 105 μM. These findings could provide starting points for the design of more potent molecules that rescue mutant p53 proteins.

More recently, compound **14**[60] (SCH529074, Figure 14) was identified from a chemical library using a screen based on p53

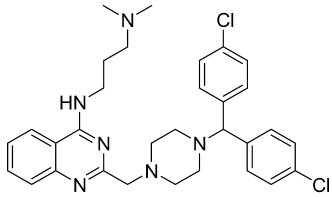

SCH529074 (14)

Figure 14. Structure of **14**.

DNA binding. Compound **14** was shown to bind specifically to the p53 DBD in a saturable manner with an affinity of 1−2 μM. Compound **14** promotes the DNA binding activity of mutant p53 both in cell-free systems and in tumor cells. Using a ^{3}H-radiolabeled analogue of compound **14**, it was shown that this compound binds to the p53 core domain, leading to an increase in the stability and rigidity of p53 DBD which interferes with HDM2 docking, thus inhibiting HDM2-mediated ubiquitination. Interestingly, the authors reported that general ubiquitination was not inhibited by compound treatment.

SOD1

Copper−zinc superoxide dismutase (SOD1) is a detoxifying enzyme localized in the cytosol, nucleus, peroxisomes, and mitochondria. SOD1 exists as a 32 kDa homodimer held together with a hydrophobic surface area that reduces the solvent accessible surface area, thus increasing dimer stability.[61] SOD1 is one of the most stable proteins known with a reported protein melting point of 85−95 °C for the fully metalated form.[62] Each SOD1 monomer also contains two metal ions, one copper and one zinc. Both metals play structural and catalytic roles in the enzyme activity (Figure 15).

Over 100 mutations in SOD1 have been identified and are believed to be responsible for about 20% of all familial amyotrophic lateral sclerosis (FALS) cases. The clinical and pathological features of FALS and sporadic ALS (amyotrophic

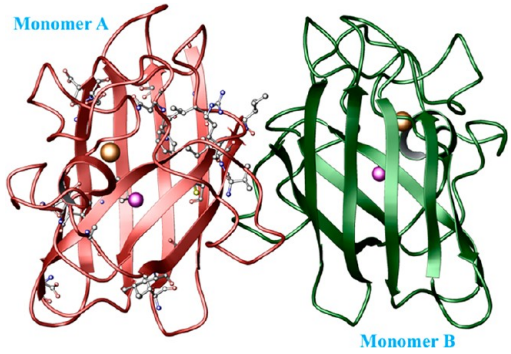

Figure 15. SOD1 WT dimer crystal structure. Monomers are represented in different colors. Cu is shown in metallic brown and Zn in magenta. All the known mutations are shown in ball and stick in monomer A. Schrodinger's Maestro[63] was used for generating this figure using PDB 1HL5 coordinates.

lateral sclerosis or Lou Gehrig's disease) are similar and result in progressive muscle loss and paralysis. Currently, there is only one FDA-approved treatment for ALS (riluzole), and that drug extends life, on average, by only 2−3 months.

Evidence suggests that mutant SOD1 protein is neurotoxic and leads to familial ALS via a GOF.[64] Studies with transgenic mice suggest that familial ALS may result from a gain of toxic function due to aggregation of the mutant form of SOD1.[65] Recent findings from Agar et al. showed that SOD1 loss of stability and propensity to aggregate are correlated with increased disease severity.[66] However, whether the final protein aggregates are themselves toxic or whether some soluble precursor is the major toxic species is the subject of hot debate.[67] SOD1 familial ALS mutations are distributed throughout the primary sequence and tertiary structure, and this is likely to affect the structural stability of SOD1. Additional SOD1 mutations have been linked to decreased metal binding,[68] decreased formation of a stabilizing intramolecular disulfide,[69] decreased structural stability, and increased propensity to monomerize[70] and aggregate both in vitro and in vivo.[71,72]

The most frequent familial ALS mutation in human SOD1, A4V, accounts for almost 50% of SOD1 linked cases and is associated with the most rapid disease progression. Interestingly, comparison of the A4V and the wild type structures revealed no significant differences in overall folding. However, it was shown that small changes at the dimer interface result in a substantial reorientation of the two monomers.[70]

Stabilization of the SOD1 dimer interface through the use of small molecules preventing protein aggregation is being pursued as a therapeutic strategy and will be discussed herein.

Small Molecule Approaches. There are no natural ligands of SOD1 to serve as a molecular scaffold for the design of small molecule stabilizers. Therefore, an in silico screening approach was applied using a library of 1.5 million commercially available small molecules to select for compounds that could potentially bind at the dimer interface and stabilize the dimer (Figure 16).[73] It was hypothesized that stabilization of the SOD1 native dimer will inhibit its aggregation regardless of the exact pathway because it will deplete the population of the aggregating species, which may be a partially unfolded apo-monomer.

Several compounds were identified by this method and displayed the ability to stabilize the A4V mutant and prevent its aggregation in vitro. In the presence of these compounds, less than 25% of the dimer had disappeared after 12 h, whereas 50%

dx.doi.org/10.1021/jm301182j | J. Med. Chem. 2012, 55, 10823−10843

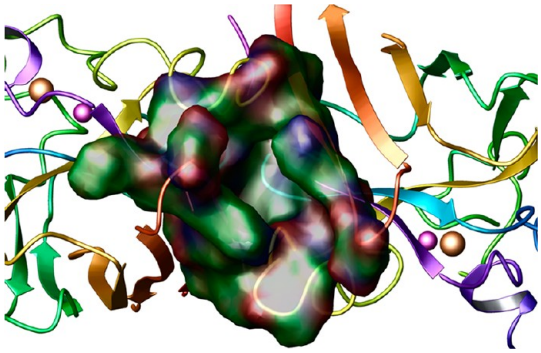

Figure 16. SOD1 dimer interface binding pocket is represented by the Connolly surface map. Cu and Zn are represented in metallic brown and magenta. Schrodinger's Maestro[63] was used to generate this figure using 1HL5 PDB coordinates.

was lost in their absence. Compounds **15**[73] and **16**[73] are examples of the reported hits and are shown in Figure 17.

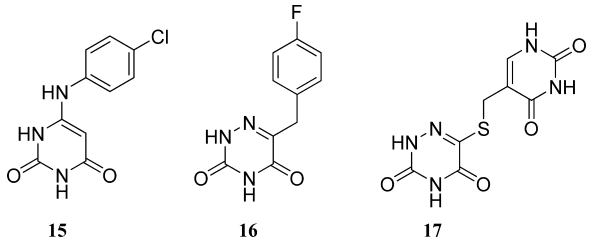

Figure 17. Examples of SOD1 hits from in silico screening.

A model for the binding of these molecules was proposed on the basis of restricted docking calculations and site-directed mutagenesis of key residues at the dimer interface.[74] A set of hydrogen bonding constraints obtained from these experiments was used to guide docking calculations of the compound library around the dimer interface. In a follow-up publication, additional hits were predicted and experimentally tested for their ability to block aggregation.[74] Six out the 14 molecules exhibited significantly high specificity of binding toward SOD1 over blood plasma components. Compound **17**[74] (Figure 17) is a representative example from the reported hits. The authors concluded that these molecules represent a new class of molecules for further optimization that could deliver potential candidate therapeutics for familial ALS.

More recently, a cellular model was developed in which cell death depended on the expression of G93A-SOD1, a mutant form of SOD1 that is found in familial ALS patients and produces toxic protein aggregates.[75] This cellular model was optimized for high throughput screening to identify protective compounds from a 50 000 member chemical library. Two hits, **18**[75] and **19**[75] (Figure 18), were identified from an arylsulfanylpyrazolone scaffold and were shown to block SOD1 aggregation in high content screening assays.

Compound **18** showed rapid clearance and poor microsomal stability. Compound **19** was found to be blood−brain barrier penetrant with a brain/plasma ratio of 0.19. The optimization of this scaffold led to the generation of analogue **20**[75] with an EC_{50} of 170 nM. Metabolite identification was performed to address the rapid clearance, and the sulfur linker was identified as a metabolic soft spot. The in vitro potency and pharmacological properties of these hits were further improved by switching to the corresponding ether analogues.[76] One of

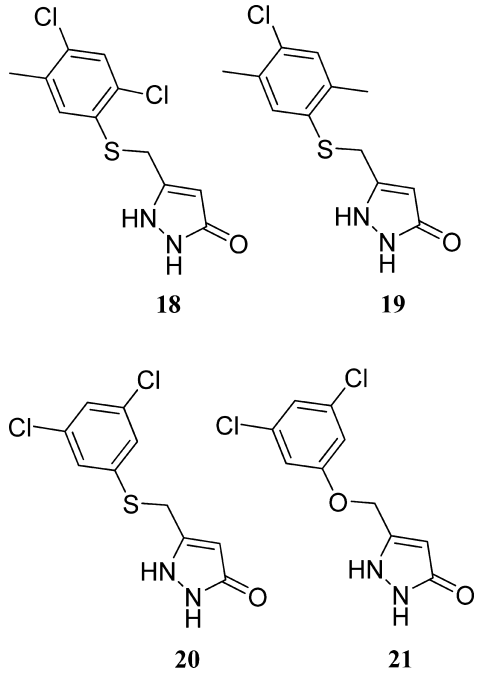

Figure 18. Examples of hits from a cell-based screen using the G93A mutant form of SOD1.

the ether analogues **21**[76] showed improved potency and ADME properties with IC_{50} = 67nM and human microsomal stability half-life of 93 min. Compound **21** also showed sustained brain levels in vivo (194 μM in brain tissue after 4 h) and a statistically significant extension in survival in the G93A ALS mice in a dose dependent manner in comparison to untreated G93A mice. The most efficacious dose (20 mg/kg) resulted in a life span extension of 13.3%.

Another scaffold was identified from the same high throughput screening assay reported above.[77] Cyclohexane-1,3-dione derivatives exemplified by compound **22**[77] (EC_{50} = 4.5 μM) are shown in Figure 19.

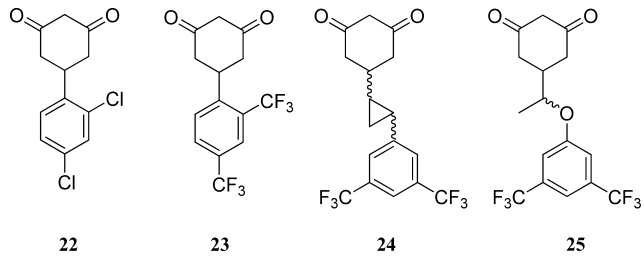

Figure 19. Cyclohexane-1,3-dione hits from a cell-based screen using the G93A mutant form of SOD1.

Additional structural modifications of the cyclohexanedione hits led to the discovery of a slightly more potent analogue **23**[77] (EC_{50} of 700 nM) (Figure 19). **23** showed good ADME properties, such as solubility (≥500 μM), high human and mouse microsomal stability (both $T_{1/2} \geq 180$ min), and high oral bioavailability (89% in Sprague−Dawley rats). **23** was also found to penetrate the blood−brain barrier. However, compound **23** did not exhibit any significant life span extension in the ALS mouse model. Although **23** was active in PC12 cells, it had poor activity in other cell types, including primary cortical neurons. Further structural modifications aimed at

dx.doi.org/10.1021/jm301182j | J. Med. Chem. 2012, 55, 10823−10843

improving the profile of compound **23** yielded racemic analogues **24**[77] and **25**[77] (Figure 19) both with IC_{50} = 700 nM in the PC12-G93A cell-based assay. **24** and **25** were reported to show consistent positive results in cortical neurons. Compound **25** was reported to have a microsomal stability $T_{1/2}$ = 71 min, good plasma stability ($T_{1/2}$ > 60 min), and an attractive efflux ratio. These cyclohexanedione analogues are being considered further as potential novel therapeutic candidates for ALS.[47]

Agar et al. presented an alternative approach to stabilize the SOD1 dimer by chemically cross-linking two adjacent cysteine residues on each respective monomer.[78] By use of two different SOD1 mutants (G93A and G85R), maleimide and thiol−disulfide exchange-mediated stabilization was observed with an optimum chain length of 8 to 14 Å (see compound **26**[78] in Figure 20).

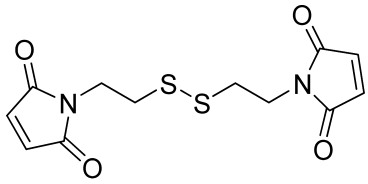

26

Figure 20. Maleimide analogue **26** stabilizes mutant SOD1.

Stabilization was measured as a function of thermal shifts. A thermal shift of 20−45 °C was observed, which represents some of the largest increases in SOD1 stability reported in the literature. The reported maleimide analogue **26** does not display favorable druglike properties which may complicate the interpretation of the data. However, the impressive increase in the thermal stability of SOD1 could pave the way to novel strategies for the stabilization of SOD1 and potentially offer opportunities for the development of new ALS treatments.

LYSOZYME

Human lysozyme was discovered in 1922 by Fleming when he noted a substance in the nasal mucus of a patient suffering from a common cold that could kill certain bacteria.[79] Since then, lysozyme has been widely studied and has been a model for investigations on protein structure and function. In fact, lysozyme isolated from hen egg-whites was the first enzyme to succumb to three-dimensional structure elucidation.[80,81] The human lysozyme contains 130 residues and is highly expressed in hematopoietic cells and is also found in granulocytes, monocytes, and macrophages.[82] It is widely distributed in a variety of tissues and body fluids, including the liver, articular cartilage, plasma, saliva, tears, and breast milk.[81] The function of lysozyme is to hydrolyze the β-1,4 glycosidic linkages between *N*-acetylmuramic acid and *N*-acetylglucosamine that occur in the peptidoglycan cell wall structure of microorganisms, particularly of Gram-positive bacteria.[83]

In 1993, Pepys and co-workers discovered that point mutations in human lysozyme correlated with hereditary systemic amyloidosis.[84] Hereditary systemic amyloidosis is a GOF disease, since it is caused by the aggregation of misfolded lysozyme into amyloids. Amyloidosis represents a disorder where there are extracellular protein aggregates that form a distinctive fibrillar structure, namely, amyloid. *Systemic* amyloidosis means that the amyloids can be seen in any or all of the viscera, connective tissue, and walls of blood vessels. Some forms of *hereditary* systemic amyloidosis are caused by a mutation in the amyloid-prone protein[85] and are characterized by the deposition of lysozyme fibrils in the kidneys, gastrointestinal tract, lymph nodes, blood vessels, spleen, and liver, sometimes in kilogram quantities.[86] Renal dysfunction[83] and hepatic hemorrhage[87] are two severe clinical features. The distribution of amyloid throughout the tissues and the age at which the amyloids forms are highly variable both within and between families, but the outcome of hereditary systemic amyloidosis is always serious and usually fatal. Therefore, an understanding of how the point mutations lead to misfolding and amyloid formation is crucial for the design of small molecules to treat this disease.

There have been numerous lysozyme crystal structures exploited to assist in the elucidation of the mechanism of mutant lysozyme aggregation.[88−91] The native structure of human lysozyme comprises two closely interacting domains, the α-helical domain and the β-sheet domain. Additionally, there are four disulfide bonds, two of which are located in the α-helix region, one in the β-sheet region, and one that connects the two domains. The active site of lysozyme is the cleft that is formed between the two domains.[92] To date, there have been six natural lysozyme mutations or combinations of mutations that have been linked to the development of hereditary systemic amyloidosis, namely, I56T, F57I, F57I/T70N, W64R, D67H, and T70N/W112R. All but one of these mutations are located on the β-sheet domain, and the locations of these mutations are shown in Figure 21.

Liu and colleagues have shown that the human lysozyme variants I156T, D678H, and T70N, the most common mutants associated with hereditary systemic amyloidosis, are more sensitive to acid or heat destabilization than is the wild type protein.[93] Additionally, these mutants unfold 3−160 times faster than WT lysozyme.[94] X-ray crystallography has shown

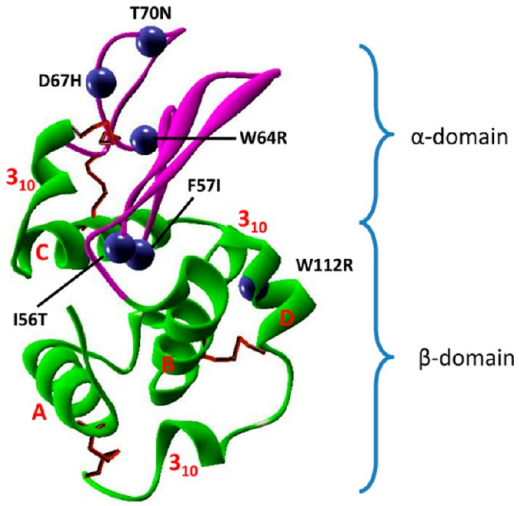

Figure 21. Representation of the wild type lysozyme structure showing location of the naturally occurring mutations. The α-domain is represented in green consisting for four α-helices labeled A−D and three 3_{10}-helices. The β-domain is represented in magenta. Intramolecular disulfide bonds between C65−C81, C77−C95, C30−C116, and C6−C128 (from top to bottom) are highlighted by red sticks. The blue spheres represent naturally occurring mutants. Note: T70N and W112R are not associated with disease. PDB code 1LOZ was used to generate the representation in Discovery Studio.[49]

dx.doi.org/10.1021/jm301182j | *J. Med. Chem.* 2012, 55, 10823−10843

Table 1. Acridine Analogues with Reported Inhibition of Lysozyme Aggregation

Acridine	Structure	IC_{50} (uM)	Acridine	Structure	IC_{50} (uM)
27	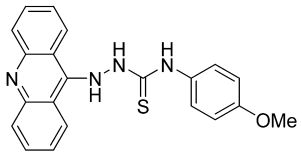	89.1	**31**	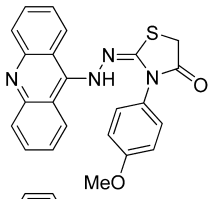	57.8
28	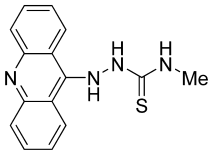	9.9	**32**	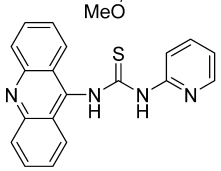	48.6
29	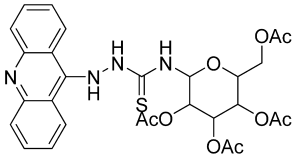	75.6	**33**	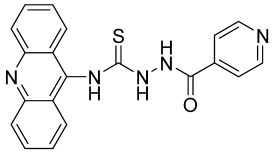	182.1
30	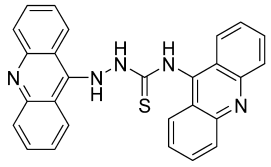	6.5	**34**	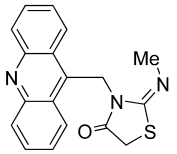	>200

that the overall folding of the mutant proteins I156T, D678H, and T70N is very similar to that of WT, with all the disulfide bonds formed correctly.[95] However, these mutations cause a loss in a number of long-range interactions that bridge the α/β domain interface, suggesting that the interface region of these mutant proteins is significantly destabilized when compared with WT.[96] Hydrogen−deuterium exchange experiments followed by NMR and MS analyses show that both the I56T and the D67H variants, but not the WT protein, populate a partially unfolded species under physiological conditions.[97] It is hypothesized that these partially unfolded intermediates can then interact with each other to initiate the aggregation phenomenon that ultimately leads to the formation of amyloid fibril.[98] This mechanism was originally proposed by Booth,[96] who suggested that a partially unfolded transient population of mutated lysozyme protein undergoes a helix-to-sheet transition and creates the first template (or seed) for further fibril formation.

To correct lysozyme aggregation, a pharmacological chaperone approach has been considered. This method involves identifying a small molecule that could enter the cell to serve as a molecular scaffold for the misfolded mutant intermediate. The goal of the "pharmacological chaperone" is to help the protein fold correctly and then traffic efficiently. The use of small molecules to correct lysozyme misfolding was examined in Gazova's laboratory,[99,100] and compounds hypothesized to bind to the β-sheets of misfolded lysozyme were investigated. Gazova and co-workers followed up on acridine-based compounds that had previously been reported in the literature as defribillization molecules.[101] Their group screened 19 acridines for their ability to prevent lysozyme aggregation at 200 μM. The acridines were divided into three groups based on their structures: planar acridines, spiroacridines, and tetrahydroacridines. The only class that was found to inhibit lysozyme aggregation was the planar acridines, while the spiro- and tetrahydroacridines were found to have no effect on inhibiting lysozyme fibrillization. The ability of the planar acridines to prevent amyloid formation was measured using a thioflavin T (ThT) fluorescence assay. The two most potent compounds, **28**[101] and **30**,[101] were found to have IC_{50} < 10 μM, as shown in Table 1.

The authors presume that the flat heterocyclic skeleton of the planar acridine allows it to intercalate between the hydrophobic residues, thereby interrupting the interface between the two neighboring β-sheets of misfolded lysozyme proteins. Additionally, since the compound with the lowest IC_{50} is the acridine dimer, **30**, it is proposed that the duplication of heterocycles simply increases the capacity of the compound to interact with protein, leading to a more effective blockage of β-sheet formation.[98] This theory is supported by the loss of anti-amyloid activity when moving from planar acridines to the more bulky, three-dimensional spiroacridines. In a more recent manuscript by these authors, the two most efficacious planar acridines were also evaluated in a cell viability assay and a DNA intercalation assay.[99] Not surprisingly, some of the acridines were found to interact with DNA, and yet the most potent inhibitor of lysozyme aggregation, **30**, did not show any DNA intercalation. These planar acridines have proven to be useful tools to study the aggregation of lysozyme.

Currently, there are no small molecules that correct lysozyme misfolding in the clinic. Perhaps the most advanced molecule known to inhibit lysozyme aggregation is a camelid antibody that binds to the amyloidogenic variants of human lysozyme.[102] Original studies showed that a nanobody, namely, cAb-HuL22, bound to the active site of human lysozyme. In order to increase the stability, a variant containing an extra disulfide bridge was designed and synthesized. This extra disulfide bond increased the stability so that the antibody was functional under the conditions used to form lysozyme fibrils in vitro. The engineered antibody was found to completely inhibit the

dx.doi.org/10.1021/jm301182j | J. Med. Chem. 2012, 55, 10823−10843

aggregation and fibril formation of both the I56T and D67H lysozyme variants in vitro. This work supports the notion that molecular targeting of amyloidogenic lysozyme is an effective strategy for inhibiting its self-assembly process. The cocrystal complex of the camelid antibody with hen lysozyme, as shown in Figure 22, confirms that the antibody binds in the enzyme active site of the mutant lysozyme. Camelid antibodies[103] can be used as structural probes for investigating the mechanism of lysozyme aggregation and may potentially have use as therapeutics to inhibit fibril formation.

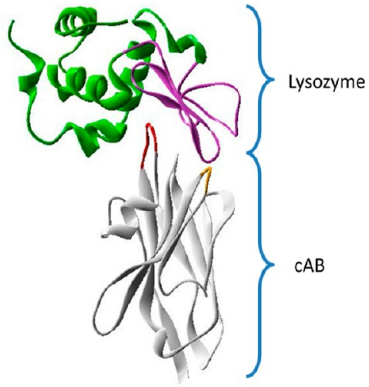

Figure 22. Ribbon diagram of lysozyme interacting with the antibody between the α and β domains. α- and β-Domains are represented by green and magenta ribbons, respectively. Camelid antibody is shown in white, and CDR3 and CDR2 loops that interact with the lysozyme are highlighted in red and yellow. The structure of the complex was generated from its X-ray coordinates (PDB code 1MEL) and was produced using Discovery Studio.[49]

SERUM AMYLOID A (SAA)

Human serum amyloid A (SAA) is an apolipoprotein comprising 104 amino acids that is predominantly produced by the liver. It associates with the carrier protein, high-density lipoprotein (HDL), for transport into the serum where it plays an important role in cholesterol circulation.[104] Some isoforms of SAA are expressed only in response to inflammatory stimuli: these are known as acute phase SAA. Acute phase serum amyloid A proteins are secreted during inflammation, as they are produced in response to inflammatory cytokines such as IL-1, IL-6, IL-8, and TNF-α.[105] SAA's role in response to inflammation includes both the recruitment of immune cells to inflammatory sites and macrophage lipid handling.[106]

The homeostatic concentration of SAA in serum is typically 1−3 mg/L. Yet during inflammation, the concentration of SAA can increase up to 1000-fold to a final concentration of over 1000 mg/L.[107] SAA levels return to baseline within a week of an inflammatory stimulus but will remain high for as long as the inflammatory cytokines remain active. Therefore, SAA levels are high in patients with a long-standing inflammatory disorder, such as rheumatoid arthritis, inflammatory bowel disease, and familial Mediterranean fever. In a small proportion of inflammatory disease patients (~10% or 17 000 patients in the U.S.), these sustained elevated levels of SAA can lead to misfolding of SAA. Misfolded SAA forms amyloids, a GOF disease known as amyloid A (AA) amyloidosis.[84] AA amyloidosis is also known as "secondary" or "reactive" systemic amyloidosis, since it is secondary to the underlying inflammatory disease. It is not known why only a small percentage of patients with prolonged elevated SAA levels develop AA amyloidosis. Understanding of this phenomenon is the focus of much research. The effects of genetic factors such as certain polymorphisms of SAA,[108] the involvement of mannose-binding lectin 2,[109] and the role of apolipoprotein E[110] are currently being investigated as potential contributing factors of AA amyloidosis.

The development of AA amyloidosis is always serious and is considered the most severe complication of chronic inflammatory disorders, particularly rheumatoid arthritis.[111] The main cause of morbidity and mortality of AA amyloidosis is amyloid deposition in the kidney, leading to a decline in renal function.[112] However, there is also nonselective proteinuria due to glomerular deposition, and therefore, nephrotic syndrome can develop before the progression to endstage kidney failure. SAA amyloid fibril deposits are almost always widespread at the time of symptom presentation and can be found in the gastrointestinal tract, spleen, liver, and autonomic nervous system.

The mechanism of SAA aggregation is not known. However, it has been discovered that the SAA amyloids consist mostly of N-terminal fragments, indicating that proteolytic cleavage is involved in pathogenesis. Additionally, these fragments are almost exclusively derived of the SAA1 isoform, suggesting that specific amino acids may be contributing to the misfolding propensity.[110] SAA binds to the heparin sulfate glycosaminoglycan (GAG) complex which is a common constituent of many different kinds of amyloid deposits. The SAA-heparin sulfate GAG assemblage is also believed to promote AA fibrillogenesis by serving as a scaffold for further fibril assembly.[113] Recent work has uncovered that SAA2 (92% homologous to SAA1) can be denatured from a stable hexamer to form multiple oligomeric species that then refold into a less stable but more accessible octameric species.[114] Further research is needed to elucidate the mechanism of SAA misfolding to form AA amyloids.

Since excessive amounts of SAA continue to be produced as long as the underlying inflammatory disease persists, the treatment for AA amyloidosis has typically been to control the inflammation and reduce the concentration of SAA in the blood. It has been established that if the SAA concentration in the blood is less than 10 mg/L, the level of amyloid deposits in the organs decrease and the 10 year survival rate is excellent at ~90%. On the other hand, if patients have SAA levels of 10 mg/L or higher, the 10 year survival rate was poor at ~40%.[115] It is clear that the suppression of SAA levels is the most important parameter in the treatment of AA amyloidosis.[116] The National Amyloidosis Centre in London recommends monthly monitoring of SAA levels in the blood for AA amyloidosis sufferers, since this is a vital guide to treatment. Current treatments for AA amyloidosis reduce SAA load through the use of anti-inflammatory/immunosuppressive therapies or anti-cytokine (TNF-α, IL-1β, or IL-6 blockade) therapies.[117]

For those cases where adequate suppression of SAA is not possible, an emerging treatment strategy is evolving. This approach uses a small molecule that will interact with the glycosaminoglycan (GAG) component of the SAA amyloid deposits, as it is believed that interfering with the interaction of SAA and GAG will inhibit amyloid formation. This was proven using a negatively charged sulfonated molecule that is a heparin sulfate mimetic, namely, eprosidate (**35**,[118] Figure 23). In a phase II/III trial, eprosidate was shown to prevent the

dx.doi.org/10.1021/jm301182j | J. Med. Chem. 2012, 55, 10823−10843

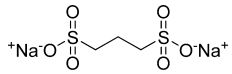

Eprodisate sodium (35)

Figure 23. Structure of **35**.

progression of nephropathy associated with AA amyloidosis without affecting SAA levels.[118] Although the treatment group showed a 42% reduction in renal decline compared to the placebo group, the amount of urinary protein excretion was not decreased. Additionally, the treatment arm had significantly more patients with chronic infections, compared with the placebo arm (21 vs 9). Therefore, the FDA requested further efficacy and safety data through additional clinical trials before approval could be given for the use of eprosidate in the treatment of AA amyloidosis. An additional international phase III study was initiated in 2010, with an estimated completion date of May 2014. The primary outcome measures of the trial will be the percent increase of serum creatinine levels in addition to percent decrease in progression to end-stage renal disease.[119]

PRIONS

Prion diseases are a group of fatal, untreatable, neurodegenerative protein-misfolding disorders, including Creutzfeldt–Jakob disease (CJD) and Gerstmann–Straüssler–Scheinker syndrome (GSS) in humans, scrapie in sheep and goat, and bovine spongiform encephalopathy (BSE) in cattle. A hallmark of prion diseases is the formation and accumulation of an aberrantly folded protein denoted scrapie prion protein (PrP^{Sc}), which is insoluble in nonionic detergents and partially resistant to proteolytic digestion and characterized by a high content of β-sheet secondary structure. Furthermore, PrP^{Sc} has the propensity to form amyloid plaques in the diseased brain.[120]

Formation of aberrantly folded protein conformers is also a hallmark of other neurodegenerative diseases, including Alzheimer's disease, Parkinson's disease, and polyglutamine disorders. However, prion diseases are unique because the pathology can be transmitted by an infectious process. The widely accepted prion hypothesis suggests that PrP^{Sc} is the main component of the infectious agent and propagates by autocatalytically converting the native protein (PrP^{C}) into the misfolded form (Figure 24A and Figure 24B).[121] Furthermore, PrP^{Sc} is able to induce misfolding of PrP^{C} in vitro resulting in the generation of prion infectious material in a test tube in the absence of living cells.[122]

No effective therapy currently exists for the prevention of infection or disease progression;[123] however, several approaches have been considered to potentially interfere with this process. Compounds that stabilize the native protein PrP^{C} and make the conformational change energetically less favorable[124] could be useful in blocking the formation of PrP^{Sc}. Alternatively, compounds that destabilize PrP^{Sc} by rendering it protease sensitive and enhance its clearance or compounds that bind to PrP^{Sc} and prevent it from serving as a template for replication could be effective. This scenario has been suggested as the mechanism of action of Congo red.[125] Another strategy might be to prevent the formation of molecular complexes by interfering with the interactions between PrP^{C} and PrP^{Sc} (Figure 24C and Figure 24D).

Several medicinal chemistry programs reported small molecules that bind to PrP^{C} and stabilize it against conversion

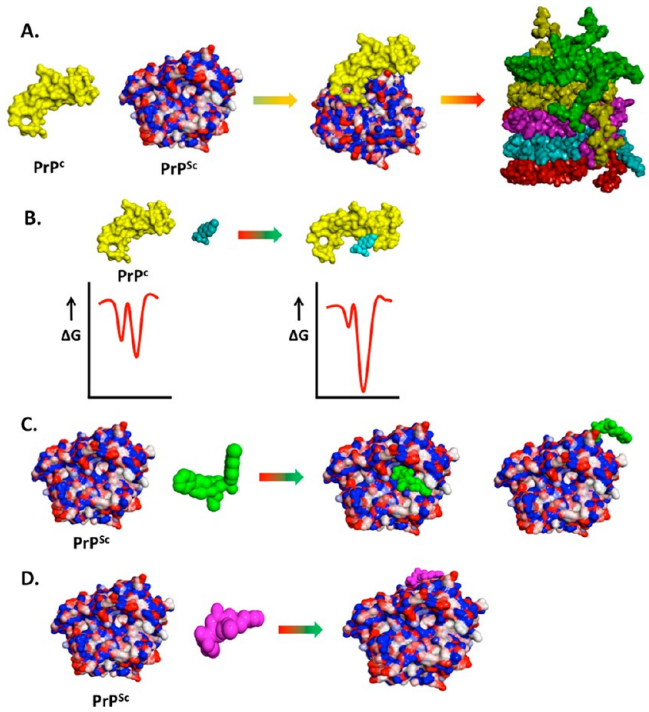

Figure 24. (A) Representation of PrP^{c} and PrP^{Sc} protein–protein interaction leading to a conformational change and amyloid plague formation. (B) Small molecule binding to PrP^{c}, stabilizing the native protein PrP^{C} and making the conformational change energetically less favorable. (C) Compounds binding to the non protein–protein interaction site of PrP^{Sc}, thereby destabilizing the conformation or tagging them for clearance. (D) Compounds binding at the protein–protein interaction site and preventing interaction with PrP^{c}.

to PrP^{Sc}, with the aim of identifying novel prion disease therapeutics. Prusiner et al.[126] conducted a computational search on the Available Chemicals Directory for molecules that mimic the dominant negative inhibition of prion replication by polymorphic variants of PrP. These authors previously showed[127] that residues Q168, Q172, T215, and Q219 on the surface of the PrP^{C} molecule contribute most prominently to the stability of the molecular complex between PrP^{C} and partner proteins, thus defining a plausible pharmacophore target for mimetic design. The compounds were screened in a cellular assay for prion replication. Pyridine dicarbonitriles **36**–**39**[127] (Figure 25), inhibited PrP^{Sc} formation in a dose-dependent manner, albeit at high concentrations (IC_{50} range from 18 to 60 μM).

Additional optimization around this scaffold led to the identification of compounds **40**, **41**, and **42**[128,129] (Figure 26)

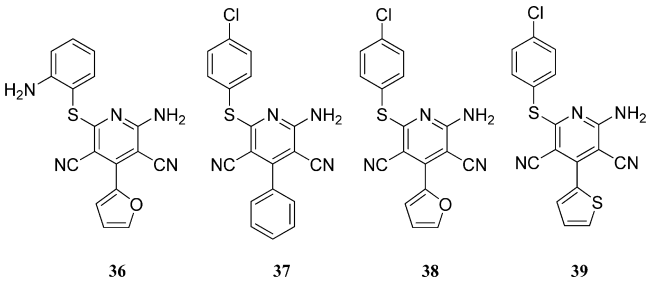

36 37 38 39

Figure 25. Pyridine dicarbonitriles with activity in cells derived from mouse ScN2a.

dx.doi.org/10.1021/jm301182j | J. Med. Chem. 2012, 55, 10823–10843

with improved potency compared to compound **36** and were found to reduce PrP^{Sc} levels to below 30% relative to an untreated control at 50 nM.

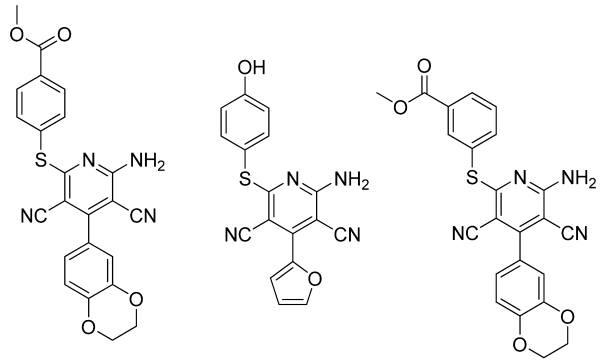

Figure 26. Structures of **40**, **41**, and **42**.

Bolognesi et al. reported the identification of novel bifunctional diketopiperazine (DKP) derivatives **43** and **44**[130] (Figure 27), with an EC_{50} of 4 and 15 μM, respectively, against

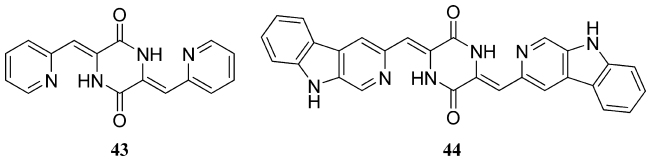

Figure 27. Structures of prion replication inhibitors **43** and **44**.

prion replication in ScGT1 cells while showing low cytotoxicity. The planar conformation of this scaffold was believed to be the major determinant for activity in this class of compounds. Studies aimed at assessing the mechanism-of-action showed that **43** might interact directly with recombinant prion protein to prevent its conversion to the pathogenic misfolded prion protein (PrP^{Sc})-like form.

ARGININE VASOPRESSIN RECEPTOR 2 (AVPR2 OR V2R)

Arginine vasopressin receptor 2 (abbreviated as AVPR2 or V2R) is a receptor for arginine vasopressin (AVP).[131] AVP is a pituitary gland nonapeptide hormone (sequence, CYFQRNCPRG-NH2). AVP is released from the posterior pituitary and has two principal sites of action: the kidney and the blood vessels. AVP's most critical function is to regulate free water reabsorption in the kidney, as the binding of AVP to V2R stimulates mechanisms that concentrate the urine and maintain water homeostasis in all organisms.[132−135]

V2R is a 371 amino acid protein belonging to the subfamily of G-protein-coupled receptors (GPCRs), class A. This receptor is a typical representative of this superfamily, built of seven transmembrane helices assembled by three extracellular loops and three intracellular loops.[136] There is no crystal structure of V2R, though several molecular models have been proposed.[137,138] To date, there have been more than 200 distinct V2R mutations identified.[139] Approximately 50% of the mutations are missense (a single amino acid swap), and the remainders comprise deletion or premature termination codon (PTC) mutations. No matter the genetic mutation, the resulting mutant V2R is nonfunctional and is therefore not able to relay the antidiuretic action of vasopressin. It has been determined that the reason for mutant V2R's lack of function (LOF) is due to an insufficient concentration of cell-surface V2R.[140] Because of the misfolding of mutant V2R, it is unable to traffic from the ER to the Golgi apparatus, and therefore, mutant V2R does not reach the cell surface, its site of action.[141]

The LOF of mutant V2R causes a disease known as nephrogenic diabetes insipidus (NDI), which occurs in ∼1 in 250 000 individuals.[142] Affected patients are unable to efficiently concentrate their urine, resulting in the excretion of large volumes of hypotonic urine (up to 25 L/day).

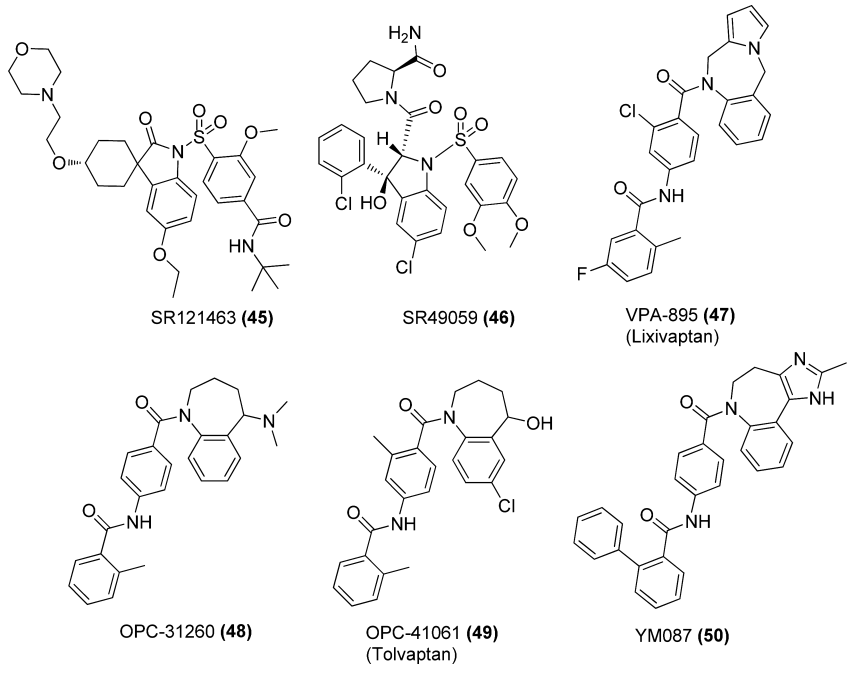

Figure 28. Structures of V2R antagonists **45**−**50**.

dx.doi.org/10.1021/jm301182j | J. Med. Chem. 2012, 55, 10823−10843

Additionally, if sufficient quantities of water are not consumed, NDI patients can have severe episodes of dehydration with serious clinical manifestations.[143] The occurrence of repeated episodes of dehydration in children may lead to mental retardation and growth disorders.

Recently, a review that compiles all of the V2R mutations and their propensity to cause NDI was published.[144] These researchers found three types of V2R mutations that result in LOF and hence cause NDI. Type I mutations result in receptors that reach the cell surface but display impaired ligand binding and are unable to induce normal water absorption. Type II mutants have defective intracellular transport so that they cannot reach the cell surface and are trapped in the interior of the cell. Type III mutant receptors were inappropriately transcribed, leading to unstable mRNA that was rapidly degraded. It was determined that the vast majority of the mutations causing NDI are type II or trafficking mutations.[132,145]

In order to increase the trafficking of a misfolded protein from the ER to the required site of action, a pharmacological chaperone approach may be used. A pharmacological chaperone is a cell permeable, small molecule that has the potential to specifically bind to folding intermediates of mutated proteins, conferring enhanced thermodynamic stability and facilitating proper transport through the secretory pathway to the correct site of action.[146] With this in mind, it was hypothesized that known V2R binders may act as pharmacological chaperones. In the first study probing this hypothesis, the rescue of cell surface mutant V2R for several mutants studied was achieved using a known V2R binder and antagonist, SR121463, **45**[144] (Figure 28). Since then, additional V2R antagonists SR49059 (**46**),[147,148] VPA-895 (**47**),[149] OPC-31260 (**48**),[149] OPC-41061 (**49**),[149] and YM087 (**50**)[149] (Figure 28) have been found to act as pharmacological chaperones, increasing functional cell surface V2R for several NDI V2R mutants.[150−152]

These V2R antagonists are believed to function as selective pharmacological chaperones by binding to the mutant receptor, stabilizing it, and thereby allowing it to traffic to the cell surface.[153] Other membrane-permeable GPCR antagonists that do not bind to V2R did not rescue cell surface expression of the NDI V2R mutants, corroborating that the compounds need to bind to the mutant receptor to promote its release from the ER. A broad subset of V2R mutations, 25 to date, have been rescued by these pharmacological chaperones.[152] Importantly, these small molecule chaperones have been shown to rescue V2R functional activity in MDCK kidney cells.[154]

V2R antagonists can restore cell surface concentration and function of NDI V2R mutants, suggesting clear therapeutic implications for NDI patients. In fact, the use of pharmacological chaperones for the treatment of NDI was recently validated in a clinical trial using **46**.[147] This study examined whether administration of **46** could restore vasopressin responsiveness in five NDI patients harboring three distinct mutations (del62-64, W164S, and R137H). After 3 days of treatment with **46**, there was a 30% reduction in urine output and up to a 40% increase in urine osmolality, without affecting sodium, potassium, creatinine excretion, or plasma sodium levels. Unfortunately, the trial was cut short because of a potential hepatoxicity observed in a separate clinical trial being conducted with **46** for a different indication. Despite the trial ending prematurely, this study provided a clear proof of concept that vasopressin antagonists may be used as pharmacological chaperones to restore mutant V2R function and treat NDI.

■ α-1-ANTITRYPSIN (A1AT)

α-1-Antitrypsin (A1AT) is a 55 kDa glycoprotein and is a member of the serine proteinase inhibitor (serpin) family of proteins. A1AT is mainly synthesized in the liver and is subsequently released into the plasma, where it is the most prevalent circulating protease inhibitor. It provides an antiprotease shield throughout the body. However, A1AT is most important in the lungs, since uncontrolled neutrophil elastase (NE), a proteolytic enzyme from the neutrophil, is capable of degrading most of the connective tissue components in the lung. A1AT is the key inhibitor of NE in the blood, and therefore, A1AT deficiencies cause serious lung disorders.

It is estimated that there are ∼200 000 patients worldwide with A1AT deficiency.[155] The deficiency of circulating A1AT is due to the misfolding of a mutated variant of A1AT, with the most common mutation being the Z variant, glutatamic acid to lysine at position 342 (E342K) of the mature protein. This single point mutation causes the protein to fold incorrectly and accumulate as a polymer in the endoplasmic reticulum (ER) of liver cells instead of being trafficked to the plasma as a functional enzyme. ZA1AT accumulation results in an 85−90% reduction of serum concentrations of A1AT.[156] The aggregates in the ER, specifically called periodic acid Schiff (PAS) positive inclusions, cannot be degraded and therefore cause serious liver damage. Currently the only curative treatment for this cirrhosis is liver transplantation. Therefore, the mutation causing A1AT deficiency results in both gain and loss of function (GOF and LOF) consequences, i.e., juvenile hepatitis, cirrhosis, or hepatocellular carcinoma due to the liver aggregates, and COPD or early onset emphesyma due to the lack of antiprotease protein in the plasma/lung.[157]

The mechanism of ZA1AT protein polymerization has been studied and characterized in detail.[158,159] Nonmutated A1AT has 3 β-sheets (A−C) and an exposed mobile reactive center loop (RCL) that presents a peptide sequence to the protease, NE, as shown in Figure 29A. After cleavage by NE, A1AT is inactivated by a remarkable conformation change that moves the RCL 70 Å, where the loop becomes an extra strand in β-sheet A (Figure 29B).[160] This extraordinary mobility is central to the inhibitory activity of A1AT. The Z mutation occurs at the head of the fifth strand of the A-sheet and the base of the mobile RCL, perturbing the relationship between the mobile loop and the β-sheet A, which results in an unstable intermediate. The unstable intermediate then forms polymers when the RCL of one A1AT molecule inserts into the β-sheet A of another A1AT protein (Figure 29C). This process continues until large polymers have been formed.

The current standard of care for A1AT deficiencies is enzyme replacement therapy (ERT).[162] There is currently no long-term clinical data showing that AIAT ERT reduces the rate of decline of lung function, and therefore additional phase IV studies are ongoing.[163] More importantly, ERT does not address the accumulation of polymer in the liver. Therefore, there have been efforts to identify small molecules that prevent polymer formation and allow ZA1AT to enter the serum, where it still retains ∼80% of its functional utility.[164,165]

One approach has been to identify a small molecule that binds strand 4 of β-sheet A of ZA1AT in order to prevent the binding of a second ZA1AT's RCL, hence preventing polymerization. Toward this end, several groups have worked

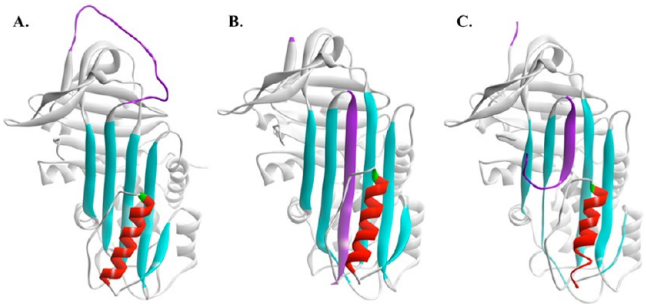

Figure 29. (A) Structure of the active form of α-1-antitrypsin. The active loop that interacts with trypsin is shown in magenta. Five β sheets are represented in the cyan, and the α helix is in red. The structure of the active α-1-antitrypsin was generated from its X-ray coordinates (PDB code 1HP7) and produced using Discovery Studio.[49] (B) Inactive stable form of α-1-antitrypsin structure. The active loop integrates itself into the β sheets. The stable inactive structure was generated from its X-ray coordinates (PDB code 3NDF) and produced using Discovery Studio.[49] (C) Inactive unstable aggregate forming α-1-antitrypsin structure. The active loop is partially integrated into the β sheet, and the other half extends to interact with another α-1-antitrypsin to form aggregate. The structure was generated from the simulation using MOE software package[161] of the inactive stable structure (derived from PDB code 3NDF) and produced using Discovery Studio.[49]

to identify β-sheet A binders/stabilizers. In 2000, Perlmutter and co-workers identified that glycerol reduced the polymerization of ZA1AT and increased the secretion of the Z variant in a cell culture model of disease.[166] This work was confirmed by the Lomas group, who also discovered additional alcohols conferring that same activity.[167] As shown in Figure 30, they

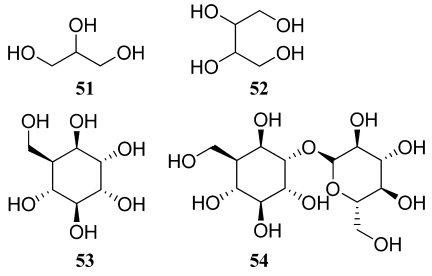

Figure 30. Structures of glycerol **51**, erythritol **52**, glucose **53**, and trehalose **54**.

found that glycerol (**51**),[167] erythritol (**52**),[167] glucose (**53**),[167] and trehalose (**54**)[167] could all similarly reduce the rate of polymerization by approximately 2.5-fold when added to the experimental buffer at ~1 M.

The mechanism of polymer reduction by these polyols is hypothesized to be the result of binding to the β-sheet A of ZA1AT. Support for this comes from a report describing how flash-cooling antithrombin crystals with glycerol introduced a glycerol molecule into the protein, where it was found to bind to β-sheet A.[168] This work served as a proof of concept for targeting the β-sheet A with a small molecule to prevent polymerization. The potential binding site of glycerol in the β-sheet A of Z A1AT is represented by the pink sphere in Figure 31.

A known chemical chaperone, 4-phenylbutyrate (4-PBA, **55**,[164] Figure 32), was found to increase secretion of ZA1AT from cells in a tissue culture, as well as in a mouse model of

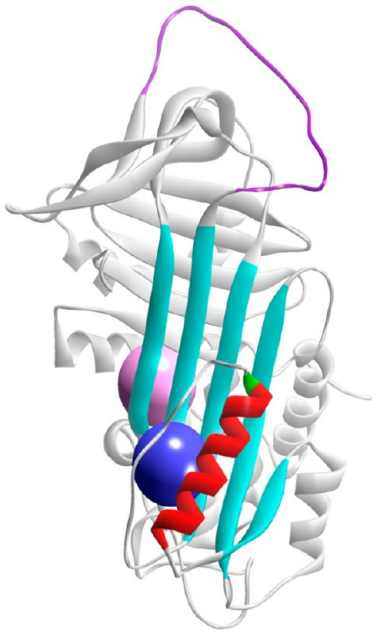

Figure 31. α-1-Antitrypsin structure with selected binding pockets highlighted. The pink region is the glycerol binding pocket, and the blue sphere represents the allosteric pocket between the α-helix and β-sheets. The active structure of α-1-antitrypsin was generated from its X-ray coordinates (PDB code 1HP7). The binding sites were identified, and the representation was generated using Discovery Studio.[49]

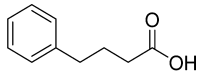

4-BPA (**55**)

Figure 32. Structure of **55**, which failed to increase circulating ZA1AT in the clinic.

ZA1AT deficiency.[164] 4-Phenylbutyrate increases ZA1AT secretion without increasing de novo protein synthesis or decreasing ER degradation. Moreover, since 4-BPA had already been approved by the FDA for the management of urea cycle disorders, it was examined in a clinical trial to probe its efficacy in treating A1AT deficiency. The trial monitored circulating levels of ZA1AT in 10 A1AT deficient patients. In this trial, **55** was not found to be effective in increasing ZA1AT levels in blood when dosed at 600 mg/day for 14 days.[169]

An alternative approach to increase circulating ZA1AT levels was pursued by Lomas and co-workers.[170] Their goal was to discover a small molecule that could prevent polymerization by binding to a region of ZA1AT that is completely distinct (remote) from the 4 position of β-sheet A, since that binding site is critical for the inhibitory function of A1AT.[159] In crystal structures of A1AT, a hydrophobic pocket had previously been identified, as indicated by the blue sphere in Figure 29.[171] Proof that targeting this pocket could result in both a decrease of polymerization and an increase of secretion of ZA1AT came from mutating an amino acid in this region that filled the cavity (T114F). With this mutation, less polymerization occurred and an increase of ZA1AT was detected in the serum.[172] However, it was unknown if the allosteric pocket could be filled by a small molecule in order to elicit the same effect.

Toward that end, Lomas conducted a virtual screen of 1.2 million commercial and druglike compounds in search of a

dx.doi.org/10.1021/jm301182j | J. Med. Chem. 2012, 55, 10823−10843

compound that would fit the hydrophobic allosteric cavity identified on ZA1AT. From the screen, 68 small molecules were selected for analysis in vitro. Most of the compounds identified by the screen did not antagonize the polymerization of ZA1AT in vitro, and some compounds even accelerated the polymerization process. However, compound **56**[170] (Figure 33)

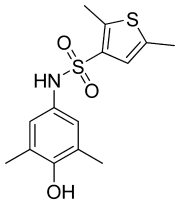

56

Figure 33. Allosteric inhibitor, **56**, prevents polymerization and increases clearance of mutant ZA1AT.

completely blocked polymerization in vitro at 200 100 50 ,and 20 μM. Although **56** reduced the retention of ZA1AT in murine liver cells by 70% when compared with controls, it was determined that there was no increase in the secretion of ZA1AT from the ER. Moreover, the **56**/ZA1AT complex was deemed to be very stable, with a melting temperature of 100 °C compared to 54.1 °C of ZA1AT alone, thus potentially compromising the functional activity of ZA1AT.

Perhaps the most advanced approach to ameliorating ZA1AT polymerization is the use of small peptides. A tetrapeptide, Ac-Thr-Thr-Ala-Ile-NH_2, has been reported as the most tight-binding ligand for ZA1AT.[173] Previous studies had shown that 11- to 13-mer synthetic peptides could bind to the β-sheet A of ZA1AT to prevent polymerization.[174] However, the molecular size and promiscuity of these larger peptides limit their therapeutic potential. The tetrapeptide was discovered using combinatorial peptide synthesis library of 10 000 peptides and was found to abolish ZA1AT polymerization in vitro. A model has been able to predict the binding of Ac-Thr-Thr-Ala-Ile-NH_2 to ZA1AT, and it is proposed that the peptide inserts into the lower part of strand 4 in the β-sheet A. Unfortunately, even though this peptide prevents ZA1AT polymerization, it also precludes its activity. Therefore, as a therapeutic, such a peptide could be used to prevent amyloidosis of the mutant A1AT but would have to be coadministered with ERT in order to have the requisite concentration of circulating functional A1AT. It is believed that this peptide can serve as a template to develop peptidomimetic tools (or drugs) for the treatment of ZA1AT related disorders.

There are currently no small molecule stabilizers, correctors, or traffickers in the clinic for the treatment of A1AT deficiency.

CONCLUSION AND OUTLOOK

Understanding the principles of protein misfolding has led to increased insight into the underlying causes of a variety of sporadic and genetic diseases associated with gain of function and loss of function. Gaps still remain in our understanding of folding intermediates and the conformational changes associated with the transition from a native to a misfolded state. Experimental characterization of the transient states of proteins remains challenging because high-resolution structural techniques such as crystallography and NMR are not suitable for studying short-lived protein states. In either sporadic or genetic diseases, the goal is to develop pharmacological small-molecule chaperones that stabilize the proteins, restore their function, and prevent them from aggregating. At the molecular level, the type of small molecule chaperone required in a given disease depends on the structure of the protein (monomer versus dimer, tetramer, or oligomer) and on how misfolding leads to loss or gain of function. Despite the challenges mentioned above, small molecules that stabilize misfolded proteins, restore protein function, and prevent aggregation have emerged and continue to advance to the clinic and ultimately will reach the patient. Tafamidis is a kinetic stabilizer of transthyretin that addresses the underlying cause of a human amyloid disease. Future advances will provide additional insight into the exact mechanism of protein misfolding and will provide new opportunities to tackle numerous, presently incurable diseases.

AUTHOR INFORMATION

Corresponding Author

*Phone: 1-617-665-5139. E-mail: eddine.saiah@pfizer.com.

Notes

The authors declare no competing financial interest.

Biographies

Lori Krim Gavrin earned her Ph.D. from the University of Pennsylvania in 2001 in Professor Jeffrey Winkler's laboratory. She started her professional career as a medicinal chemist at Wyeth Research (now Pfizer). Over the past 11+ years, her work has spanned various stages of research from early exploratory to late discovery within multiple therapeutic areas. Lori has led teams from HTS to lead discovery and has also advanced several late stage programs. As a member of the norepinephrine reuptake inhibitor program at Wyeth, Lori designed and synthesized a compound that entered phase I clinical trials for the treatment of vasomotor symptoms. At present, Lori is leading chemistry design efforts within Pfizer's Orphan and Genetic Disease Research Unit.

Rajiah Aldrin Denny's research efforts focus on computational and cheminformatics aspects of drug discovery. During his time in Biogen-Idec, Wyeth, and currently Pfizer, he worked on diverse disease areas including inflammation, immunology, oncology, and protein misfolding. He has contributed to exploratory and late stage discovery projects using structure- and ligand-based drug design, virtual screening, and ADMET modeling. He was also involved in cheminformatics application development efforts. Denny obtained his Ph.D. from Indian Institute of Technology, Madras, India, in 1998 and received the Langmuir Best Thesis Award. His postdoctoral research focused on Raman spectroscopy, solvation dynamics, and electron transfer using statistical mechanics and MD/MC simulations at Indian Institute of Science, Bangalore, India, and Harvard University, Cambridge, MA.

Eddine Saiah received his Ph.D. from Pierre and Marie Curie University in Paris in 1992 followed by a postdoc at the Mayo Clinic Florida. He has worked at several companies, including DuPont Pharmaceuticals and Wyeth. He joined Pfizer in 2009 through the Wyeth acquisition where he was leading the Med Chem group in Cambridge, MA. He has worked on a range of programs including oncology, cardiovascular, metabolic diseases, and inflammation with multiple compounds advancing to the clinic and applied fragment-based approaches on multiple programs. He is currently working in the Orphan and Genetic Disease Research Unit with a focus on understanding and tackling protein misfolding with small molecules. He is the cochair of the Pfizer Medicinal Chemistry Design Network Group.

■ ACKNOWLEDGMENTS

The authors thank Lyn Jones and Mark Bunnage for their support during the preparation of this manuscript. We also thank Nels Thorsteinson (Chemical Computing Group, Canada) for his help with A1AT inactive unstable conformer preparation in MOE using Monte Carlo simulations.

■ ABBREVIATIONS USED

AA, amyloid A; A1AT, α-1-antitrypsin; ADME, absorption, distribution, metabolism, and excretion; ALS, amyotrophic lateral sclerosis; AVPR2, arginine vasopressin receptor 2; BSE, bovine spongiform encephalopathy; CJD, Creutzfeldt−Jakob disease; CNSA, central nervous system amyloidoses; SOD1, copper−zinc superoxide dismutase 1; CSF, cerebrospinal fluid; DBD, DNA-binding domain; ER, endoplasmic reticulum; ERT, enzyme replacement therapy; FAC, familial amyloid cardiomyopathy; FAP, familial amyloid polyneuropathy; GAG, glycosaminoglycan; GOF, gain of function; GPCR, G-protein-coupled receptor; GSS, Gerstmann−Straüssler−Scheinker syndrome; HBP, hydrophobic halogen binding pocket; HSF1, heat shock factor protein 1; HSP, heat shock protein; LOF, loss of function; NDI, nephrogenic diabetes insipidus; NE, neutrophil elastase; NMR, nuclear magnetic resonance; PDB, Protein Data Bank; PrP^{C}, native protein; PrP^{Sc}, scrapie prion protein; PRR, proline-rich region; PTC, premature termination codon; RBP, retinol binding protein; SBDD, structure based drug design; SSA, senile systemic amyloidosis; SAA, serum amyloid A; RCL, reactive center loop; TAD, terminal transactivation domain; TBG, thyroid-binding globulin; TTR, transthyretin; ThT, thioflavin T; UPR, unfolded protein response; V2R, vasopressin receptor 2; WT, wild type

■ REFERENCES

(1) Campioni, S.; Monsellier, E.; Chiti, F. Why Proteins Misfold. In *Protein Misfolding Diseases: Current and Emerging Principles and Therapies*; Ramirez-Alvarado, M., Kelly, J. W., Dobson, C. M., Eds.; John Wiley & Sons, Inc.: Hoboken, NJ, 2010; pp 3−20.

(2) Herczenik, E.; Gebbink, M. F. Molecular and cellular aspects of protein misfolding and disease. *FASEB J.* **2008**, *22*, 2115−2133.

(3) Ségalat, L. Loss-of-function genetic diseases and the concept of pharmaceutical targets. *Orphanet J. Rare Dis.* **2007**, *2*, 30−36.

(4) Ellis, R. J. Macromolecular crowding: an important but neglected aspect of the intracellular environment. *Curr. Opin. Struct. Biol.* **2001**, *1*, 114−119.

(5) Hartl, F. U.; Hayer-Hartl, M. Molecular chaperones in the cytosol: from nascent chain to folded protein. *Science* **2002**, *295*, 1852−1858.

(6) Mayer, M. P. Gymnastics of molecular chaperones. *Mol. Cell* **2010**, *39*, 321−331.

(7) Sloan, L. A.; Fillmore, M. C.; Churcher, I. Small-molecule modulation of cellular chaperones to treat protein misfolding disorders. *Curr. Opin. Drug Discovery Dev.* **2009**, *5*, 666−681.

(8) Pettit, R. S. Cystic fibrosis transmembrane conductance regulator-modifying medications: the future of cystic fibrosis treatment. *Ann. Pharmacother.* **2012**, *46*, 1065−1075.

(9) Smid, B. E.; Aerts, J. M.; Boot, R. G.; Linthorst, G. E.; Hollak, C. E. Pharmacological small molecules for the treatment of lysosomal storage disorders. *Expert Opin. Invest. Drugs* **2010**, *19*, 1367−1379.

(10) Himmelstein, D. S.; Ward, S. M.; Lancia, J. K.; Patterson, K. R.; Binder, L. I. Tau as a therapeutic target in neurodegenerative disease. *Pharmacol. Ther.* **2012**, *136*, 8−22.

(11) Lendel, C.; Bertoncini, C. W.; Cremades, N.; Waudby, C. A.; Vendruscolo, M.; Dobson, C. M.; Schenk, D.; Christodoulou, J.; Toth, G. On the mechanism of nonspecific inhibitors of protein aggregation: dissecting the interactions of alpha-synuclein with Congo red and lacmoid. *Biochemistry* **2009**, *48*, 8322−8334.

(12) Blake, C. C.; Geisow, M. J.; Oatley, S. J.; Rerat, B.; Rerat, C. Structure of prealbumin: secondary, tertiary and quaternary interactions determined by Fourier refinement at 1.8 Å. *J. Mo.l Biol.* **1978**, *121*, 339−356.

(13) Monaco, H. L.; Rizzi, M.; Coda, A. Structure of a complex of two plasma proteins: transthyretin and retinol-binding protein. *Science* **1995**, *268*, 1039−1041.

(14) Wojtczak, A.; Luft, J.; Cody, V. Mechanism of molecular recognition. Structural aspects of 3,3′-diiodo-L-thyronine binding to human serum transthyretin. *J. Biol. Chem.* **1992**, *267*, 353−357.

(15) White, J. T.; Kelly, J. W. Support for the multigenic hypothesis of amyloidosis: the binding stoichiometry of retinol-binding protein, vitamin A, and thyroid hormone influences transthyretin amyloidogenicity in vitro. *Proc. Natl. Acad. Sci. U.S.A.* **2001**, *98*, 13019−13024.

(16) Dobson, C. M. Protein folding and misfolding. *Nature* **2003**, *426*, 884−890.

(17) Selkoe, D. J. Folding proteins in fatal ways. *Nature* **2003**, *426*, 900−904.

(18) Westermark, P.; Bergstrom, J.; Solomon, A.; Murphy, C.; Sletten, K. Transthyretin-derived senile systemic amyloidosis: clinicopathologic and structural considerations. *Amyloid* **2003**, *10*, 48−54.

(19) Westermark, P.; Sletten, K.; Johansson, B.; Cornwell, G. G. Fibril in senile systemic amyloidosis is derived from normal transthyretin. *Proc. Natl. Acad. Sci. U.S.A.* **1990**, *87*, 2843−2845.

(20) Jiang, X.; Buxbaum, J. N.; Kelly, J. W. The V122I cardiomyopathy variant of transthyretin increases the velocity of rate-limiting tetramer dissociation, resulting in accelerated amyloidosis. *Proc. Natl. Acad. Sci. U.S.A.* **2001**, *98*, 14943−14948.

(21) Jacobson, D. R.; Pastore, R. D.; Yaghoubian, R.; Kane, I.; Gallo, G.; Buck, F. S.; Buxbaum, J. N. Variant-sequence transthyretin (isoleucine 122) in late-onset cardiac amyloidosis in black Americans. *N. Engl. J. Med.* **1997**, *336*, 466−473.

(22) Sasaki, H.; Yoshioka, N.; Takagi, Y. Structure of the chromosomal gene for human serum prealbumin. *Gene* **1985**, *37*, 191−197.

(23) Sekijima, Y.; Hammarstrom, P.; Matsumura, M.; Shimizu, Y.; Iwata, M.; Tokuda, T.; Ikeda, S.; Kelly, J. W. Energetic characteristics of the new transthyretin variant A25T may explain its atypical central nervous system pathology. *Lab. Invest.* **2003**, *83*, 409−417.

(24) Hammarstrom, P.; Sekijima, Y.; White, J. T.; Wiseman, R. L.; Lim, A.; Costello, C. E.; Altland, K.; Garzuly, F.; Budka, H.; Kelly, J. W. D18G transthyretin is monomeric, aggregation prone, and not detectable in plasma and cerebrospinal fluid: a prescription for central nervous system amyloidosis. *Biochemistry* **2003**, *42*, 6656−6663.

(25) Plante-Bordeneuve, V.; Said, G. Transthyretin related familial amyloid polyneuropathy. *Curr. Opin. Neurol.* **2000**, *13*, 569−573.

(26) Gambetti, P.; Russo, C. Human brain amyloidoses. *Nephrol., Dial., Transplant.* **1998**, *13* (Suppl. 7), 33−40.

(27) Plante-Bordeneuve, V.; Said, G. Familial amyloid polyneuropathy. *Lancet Neurol.* **2011**, *10*, 1086−1097.

(28) Said, G.; Grippon, S.; Kirkpatrick, P. Tafamidis. *Nat. Rev. Drug Discovery* **2012**, *11*, 185−186.

(29) Jacobson, D. R.; Pastore, R. D.; Yaghoubian, R.; Kane, I.; Gallo, G.; Buck, F. S.; Buxbaum, J. N. Variant-sequence transthyretin (isoleucine 122) in late-onset cardiac amyloidosis in black Americans. *N. Engl. J. Med.* **1997**, *336*, 466−473.

(30) Hurshman, A. R.; White, J. T.; Powers, E. T.; Kelly, J. W. Transthyretin aggregation under partially denaturing conditions is a downhill polymerization. *Biochemistry* **2004**, *43*, 7365−7381.

(31) Johnson, S. M.; Wiseman, R. L.; Sekijima, Y.; Green, N. S.; Adamski-Werner, S. L.; Kelly, J. W. Native state kinetic stabilization as a strategy to ameliorate protein misfolding diseases: a focus on the transthyretin amyloidoses. *Acc. Chem. Res.* **2005**, *38*, 911−921.

(32) Johnson, S. M.; Connelly, S.; Fearns, C.; Powers, E. T.; Kelly, J. W. The transthyretin amyloidoses: from delineating the molecular

mechanism of aggregation linked to pathology to a regulatory-agency-approved drug. *J. Mol. Biol.* **2012**, *421*, 185−203.
(33) Miroy, G. J.; Lai, Z.; Lashuel, H. A.; Peterson, S. A.; Strang, C.; Kelly, J. W. Inhibiting transthyretin amyloid fibril formation via protein stabilization. *Proc. Natl. Acad. Sci. U.S.A.* **1996**, *93*, 15051−15056.
(34) Wojtczak, A.; Cody, V.; Luft, J. R.; Pangborn, W. Structures of human transthyretin complexed with thyroxine at 2.0 angstroms resolution and 3′,5′-dinitro-*N*-acetyl-L-thyronine at 2.2 angstroms resolution. *Acta Crystallogr., Sect. D: Biol. Crystrallogr.* **1996**, *52*, 758−765.
(35) Wiseman, R. L.; Johnson, S. M.; Kelker, M. S.; Foss, T.; Wilson, I. A.; Kelly, J. W. Kinetic stabilization of an oligomeric protein by a single ligand binding event. *J. Am. Chem. Soc.* **2005**, *127*, 5540−5551.
(36) Connelly, S.; Choi, S.; Johnson, S. M.; Kelly, J. W.; Wilson, I. A. Structure-based design of kinetic stabilizers that ameliorate the transthyretin amyloidoses. *Curr. Opin. Struct. Biol.* **2010**, *20*, 54−62.
(37) Sekijima, Y.; Dendle, M. A.; Kelly, J. W. Orally administered diflunisal stabilizes transthyretin against dissociation required for amyloidogenesis. *Amyloid* **2006**, *13*, 236−249.
(38) Miller, S. R.; Sekijima, Y.; Kelly, J. W. Native state stabilization by NSAIDs inhibits transthyretin amyloidogenesis from the most common familial disease variants. *Lab. Invest.* **2004**, *84*, 545−552.
(39) Coelho, T.; Maia, L.; Martins da Silva, A.; Waddington Cruz, M.; Plante-Bordeneuve, V.; Lozeron, P. A comprehensive evaluation of the disease-modifying effects of tafamidis in patients with transthyretin type familial amyloid polyneuropathy. *Neurology* **2011**, *76* (Suppl. 4), A111.
(40) Razavi, H.; Palaninathan, S. K.; Powers, E. T.; Wiseman, R. L.; Purkey, H. E.; Mohamedmohaideen, N. N.; Deechongkit, S.; Chiang, K. P.; Dendle, M. T.; Sacchettini, J. C.; Kelly, J. W. Benzoxazoles as transthyretin amyloid fibril inhibitors: synthesis, valuation, and mechanism of action. *Angew. Chem., Int. Ed.* **2003**, *42*, 2758−2761.
(41) European Medicines Agency (EMA). European Public Assessment Report. EMA Web site, 2011. http://www.ema.europa.eu/docs/en_GB/document_library/EPAR_-_Product_Information/human/002294/WC500117862.pdf
(42) Choi, S.; Connelly, S.; Reixach, N.; Wilson, I. A.; Kelly, J. W. Chemoselective small molecules that covalently modify one lysine in a non-enzyme protein in plasma. *Nat. Chem. Biol.* **2010**, *6*, 133−139.
(43) Kolstoe, S. E.; Mangione, P. P.; Bellotti, V.; Taylor, G. W.; Tenent, G. A.; Deroo, S.; Morrison, A. J.; Cobb, A. J. A.; Coyne, A.; McCammon, M. G.; Warner, T. D.; Mitchell, J.; Gill, R.; Smith, M. D.; Ley, S. V.; Robinson, C. V.; Wood, S. P.; Pepys, M. B. Trapping of palindromic ligands within native transthyretin prevents amyloid formation. *Proc. Natl. Acad. Sci. U.S.A.* **2010**, *107*, 20483−20488.
(44) Green, N. S.; Palaninathan, S. K.; Sacchettini, J. C.; Kelly, J. W. Synthesis and characterization of potent bivalent amyloidosis inhibitors that bind prior to transthyretin tetramerization. *J. Am. Chem. Soc.* **2003**, *125*, 13404−13414.
(45) *The PyMOL Molecular Graphics System*, version 1.5.0.4; Schrödinger, LLC: New York.
(46) Brown, C. J.; Lain, S.; Verma, C. S.; Fersht, A. R.; Lane, D. P. Awakening guardian angels: drugging the p53 pathway. *Nat. Rev. Cancer* **2009**, *12*, 862−873.
(47) Olivier, M.; Hollstein, M.; Hainaut, P. TP53 mutations in human cancers: origins, consequences, and clinical use. *Cold Spring Harbor Perspect. Biol.* **2010**, 1:a001008.
(48) Cho, Y.; Gorina, S.; Jeffrey, P. D.; Pavletich, N. P. Crystal structure of a p53 tumor suppressor−DNA complex: understanding tumorigenic mutations. *Science* **1994**, *265*, 346−355.
(49) *Discovery Studio*, version 3.1; Accelrys Software Inc.: San Diego, CA, 2010.
(50) Bullock, A. N.; Henckel, J.; DeDecker, B. S.; Johnson, C. M.; Nikolova, P. V.; Proctor, M. R.; Lane, D. P.; Fersht, A. R. Thermodynamic stability of wild-type and mutant p53 core domain. *Proc. Natl. Acad. Sci. U.S.A.* **1997**, *94*, 14338−14342.
(51) Rippin, T. M.; Bykov, V. J.; Freund, S. M.; Selivanova, G.; Wiman, K. G.; Fersht, A. R. Characterization of the p53-rescue drug CP-31398 in vitro and in living cells. *Oncogene* **2002**, *21*, 2119−2129.
(52) Friedler, A.; Hansson, L. O.; Veprintsev, D. B.; Freund, S. M.; Rippin, T. M.; Nikolova, P. V.; Proctor, M. R.; Rüdiger, S.; Fersht, A. R. A peptide that binds and stabilizes p53 core domain: chaperone strategy for rescue of oncogenic mutants. *Proc. Natl. Acad. Sci. U.S.A.* **2002**, *99*, 937−942.
(53) Foster, B. A.; Coffey, H. A.; Morin, M. J.; Rastinejad, F. Pharmacological rescue of mutant p53 conformation and function. *Science* **1999**, *286*, 2507−2510.
(54) Bykov, V. J.; Issaeva, N.; Shilov, A.; Hultcrantz, M.; Pugacheva, E.; Chumakov, P.; Wiman, K. G.; Selivanova, G. Restoration of the tumor suppressorfunction to mutant p53 by a low-molecular-weight compound. *Nat. Med.* **2002**, *8*, 282−288.
(55) Bykov, V. J.; Issaeva, N.; Zache, N.; Shilov, A.; Hultcrantz, M.; Bergman, J.; Selivanova, G.; Wiman, K. G. Reactivation of mutant p53 and induction of apoptosis in human tumor cells by maleimide analogs. *J. Biol. Chem.* **2005**, *280*, 30384−30391.
(56) Zache, N.; Lambert, J. M.; Rökaeus, N.; Shen, J.; Hainaut, P.; Bergman, J.; Wiman, K. G.; Bykov, V. J. Mutant p53 targeting by the low molecular weight compound STIMA-1. *Mol. Oncol.* **2008**, *2*, 70−80.
(57) Joerger, A. C.; Ang, H. C.; Fersht, A. R. Structural basis for understanding oncogenic p53 mutations and designing rescue drugs. *Proc. Natl. Acad. Sci. U.S.A.* **2006**, *103*, 15056−15061.
(58) Boeckler, F. M.; Joerger, A. C.; Jaggi, G.; Rutherford, T. J.; Veprintsev, D. B.; Fersht, A. R. Targeted rescue of a destabilized mutant of p53 by an in silico screened drug. *Proc. Natl. Acad. Sci. U.S.A.* **2008**, *105*, 10360−10365.
(59) Basse, N.; Kaar, J. L.; Settanni, G.; Joerger, A. C.; Rutherford, T. J.; Fersht, A. R. Toward the rational design of p53-stabilizing drugs: probing the surface of the oncogenic Y220C mutant. *Chem. Biol.* **2010**, *17*, 46−56.
(60) Demma, M.; Maxwell, E.; Ramos, R.; Liang, L.; Li, C.; Hesk, D.; Rossman, R.; Mallams, A.; Doll, R.; Liu, M.; Seidel-Dugan, C.; Bishop, W. R.; Dasmahapatra, B. SCH529074, a small molecule activator of mutant p53, which binds p53 DNA binding domain (DBD), restores growth suppressive function to mutant p53 and interrupts HDM2-mediated ubiquitination of wild type p53. *J. Biol. Chem.* **2010**, *285*, 10198−10212.
(61) Goodsell, D. S.; Olson, A. J. Structural symmetry and protein function. *Annu. Rev. Biophys. Biomol. Struct.* **2000**, *29*, 105−153.
(62) Lepock, J. R.; Arnold, L. D.; Torrie, B. H.; Andrews, B.; Kruuv, J. Structural analyses of various Cu^{2+},Zn^{2+}-superoxide dismutases by differential scanning calorimetry and Raman spectroscopy. *Arch. Biochem. Biophys.* **1985**, *241*, 243−251.
(63) *Maestro*, version 9.3; Schrödinger, LLC: New York, NY, 2012.
(64) Gurney, M. E.; Pu, H.; Chiu, A. Y.; Dal Canto, M. C.; Polchow, C. Y.; Alexander, D. D.; Caliendo, J.; Hentati, A.; Kwon, Y. W.; Deng, H. X. Motor neuron degeneration in mice that express a human Cu,Zn superoxide dismutase mutation. *Science* **1994**, *264*, 1772−1775.
(65) Bruijn, L. I.; Cleveland, D. W. Mechanisms of selective motor neuron death in ALS: insights from transgenic mouse models of motor neuron disease. *Neuropathol. Appl. Neurobiol.* **1996**, *22*, 373−387.
(66) Wang, Q.; Johnson, J. L.; Agar, N. Y.; Agar, J. N. Protein aggregation and protein instability govern familial amyotrophic lateral sclerosis patient survival. *PLoS Biol.* **2008**, *6*, 1508−1526.
(67) Rakhit, R.; Chakrabartty, A. Structure, folding, and misfolding of Cu,Zn superoxide dismutase in amyotrophic lateral sclerosis. *Biochim. Biophys. Acta* **2006**, *1762*, 1025−1037.
(68) Hayward, L. J.; Rodriguez, J. A.; Kim, J. W.; Tiwari, A.; Goto, J. J.; Cabelli, D. E.; Valentine, J. S.; Brown, R. H., Jr. Decreased metallation and activity in subsets of mutant superoxide dismutases associated with familial amyotrophic lateral sclerosis. *J. Biol. Chem.* **2002**, *277*, 15923−15931.
(69) Tiwari, A.; Hayward, L. J. Familial amyotrophic lateral sclerosis mutants of copper/zinc superoxide dismutase are susceptible to disulfide reduction. *J. Biol. Chem.* **2003**, *278*, 5984−5992.
(70) Hough, M. A.; Grossmann, J. G.; Antonyuk, A.; Strange, R. W.; Doucette, P. A.; Rodriguez, J. A.; Whitson, L. J.; Hart, P. J.; Hayward, L. J.; Valentine, J. S.; Hasnain, S. S. Dimer destabilization in superoxide

dismutase may result in disease-causing properties: structures of motor neuron disease mutants. *Proc. Natl. Acad. Sci. U.S.A.* **2004**, *101*, 5976−5981.
(71) Furukawa, Y.; Torres, A. S.; O'Halloran, T. V. Oxygen-induced maturation of SOD1: a key role for disulfide formation by the copper chaperone CCS. *EMBO J.* **2004**, *23*, 2872−2881.
(72) Shaw, B. F.; Lelie, H. L.; Durazo, A.; Nersissian., A. M.; Xu, G.; Chan, P. K.; Gralla, E. B.; Tiwari, A.; Hayward, L. J.; Borchelt, D. R.; Valentine, J. S.; Whitelegge, J. P. Detergent-insoluble aggregates associated with amyotrophic lateral sclerosis in transgenic mice contain primarily full-length, unmodified superoxide dismutase-1. *J. Biol. Chem.* **2008**, *283*, 8340−8350.
(73) Ray, S. S.; Nowak, R. J.; Brown, R. H.; Lansbury, P. T., Jr. Small-molecule-mediated stabilization of familial amyotrophic lateral sclerosis-linked superoxide dismutase mutants against unfolding and aggregation. *Proc. Natl. Acad. Sci. U.S.A.* **2005**, *102*, 3639−3644.
(74) Nowak, R. J.; Cuny, G. D.; Choi, S.; Lansbury, P. T.; Ray, S. S. Improving binding specificity of pharmacological chaperones that target mutant superoxide dismutase-1 linked to familial amyotrophic lateral sclerosis using computational methods. *J. Med. Chem.* **2010**, *53*, 2709−2718.
(75) Benmohamed, R.; Arvanites, A. C.; Kim, J.; Ferrante, R. J.; Silverman, R. B.; Morimoto, R. I.; Kirsch, D. R. Identification of compounds protective against G93A-SOD1 toxicity for the treatment of amyotrophic lateral sclerosis. *Amyotrophic Lateral Scler.* **2011**, *2*, 87−96.
(76) Chen, T.; Benmohamed, R.; Kim, J.; Smith, K.; Amante, D.; Morimoto, R. I.; Kirsch, D. R.; Ferrante, R. J.; Silverman, R. B. ADME-guided design and synthesis of aryloxanyl pyrazolone derivatives to block mutant superoxide dismutase 1 (SOD1) cytotoxicity and protein aggregation: potential application for the treatment of amyotrophic lateral sclerosis. *J. Med. Chem.* **2012**, *55*, 515−527.
(77) Zhang, W.; Benmohamed, R.; Arvanites, A. C.; Morimoto, R. I.; Ferrante, R. J.; Kirsch, D. R.; Silverman, R. B. Cyclohexane 1,3-diones and their inhibition of mutant SOD1-dependent protein aggregation and toxicity in PC12 cells. *Bioorg. Med. Chem.* **2012**, *20*, 1029−1045.
(78) Auclair, J. R.; Boggio, K. J.; Petsko, G. A.; Ringe, D.; Agar, J. N. Strategies for stabilizing superoxide dismutase (SOD1), the protein destabilized in the most common form of familial amyotrophic lateral sclerosis. *Proc. Natl. Acad. Sci. U.S.A.* **2010**, *107*, 21394−21399.
(79) Fleming, A. On a remarkable bacteriolytic element found in tissues and secretions. *Proc. R. Soc. London, Ser. B* **1922**, *93*, 306−317.
(80) Blake, C. C. F.; Koenig, D. F.; Mair, G. A.; North, A. C. T.; Phillips, D. C.; Sarma, V. R. Structure of hen egg-white lysozyme: a three dimensional Fourier synthesis at 2 angstrom resolution. *Nature* **1965**, *206*, 757−761.
(81) Phillips, D. C. The three-dimensional structure of an enzyme molecule. *Sci. Am.* **1966**, *215*, 78−90.
(82) Reitamo, S.; Klockars, M.; Adinolfi, M.; Osserman, E. F. Human lysozyme: origin and distribution in health and disease. *Ricerca Clin. Lab.* **1978**, *8*, 211−231.
(83) Jolles, P.; Jolles, J. What's new in lysozyme research? *Mol. Cell. Biochem.* **1984**, *63*, 165−189.
(84) Pepys, M. B.; Hawkins, P. N.; Booth, D. R.; Vigushin, D. M.; Tennent, G. A.; Soutar, A. K.; Totty, N.; Nguyen, O.; Blake, C. C.; Teryy, C. J.; Feest, T. G.; Zalin, A. M.; Hsuan, J. J. Human lysozyme gene mutations cause hereditary systemic amyloidosis. *Nature* **1993**, *362*, 553−557.
(85) Pepys, M. B. Amyloidosis. *Annu. Rev. Med.* **2006**, *57*, 223−241.
(86) Swaminathan, R.; Ravi, V. K.; Kumar, S.; Kumar, M. V.; Chandra, N. Lysozyme: a model protein for amyloid research. *Adv. Protein. Chem. Struct. Biol.* **2011**, *84*, 63−111.
(87) Harrison, R. F.; Hawkins, P. N.; Roche, W. R.; MacHahon, R. F.; Hubscher, S. G.; Buckels, J. A. Fragile liver and massive hepatic haemorrhage due to hereditary amyloidosis. *Gut* **1996**, *38*, 151−152.
(88) Canet, D.; Sunde, M.; Last, A. M.; Miranker, A.; Spencer, A.; Robinson, C. V.; Dobson, C. M. Mechanistic studies of the folding of human lysozyme and the origin of amyloidogenic behavior in its disease-related variants. *Biochemistry* **1999**, *38*, 6419−6427.
(89) Hooke, S. D.; Radford, S. E.; Dobson, C. M. The refolding of human lysozyme: a comparison with the structurally homologous hen lysozyme. *Biochemistry* **1994**, *33*, 5867−5876.
(90) Takano, K.; Funahashi, J.; Yutani, K. The stability and folding process of amyloidogenic mutant human lysozymes. *Eur. J. Biochem.* **2001**, *268*, 155−159.
(91) Wain, R.; Smith, L. J.; Dobson, C. M. Oxidative refolding of amyloidogenic variants of human lysozyme. *J. Mol. Biol.* **2005**, *351*, 662−671.
(92) Dumoulin, M. In *Familial Amyloidosis Caused by Lysozyme in Protein Misfolding Diseases: Current and Emerging Principles and Therapies*; Ramirez-Alvarado, M.; Kelly, J. W., Dobson, C. M., Eds.; John Wiley & Sons, Inc.: Hoboken, NJ, 2010; pp 867−885.
(93) Liu, H.-L.; Wu, Y.-C.; Zhao, J.-H.; Liu, Y.-F.; Huang, C.-H.; Fang, H.-W.; Ho, Y. Insights into the conformational changes of several human lysozyme variants associated with hereditary systemic amyloidosis. *Biotechnol. Prog.* **2007**, *23*, 246−254.
(94) Esposito, G.; Garcia, J.; Mangione, P.; Giorgetti, S.; Corazza, A.; Viglino, P.; Chiti, F.; Andreola, A.; Dumy, P.; Booth, D. Structural and folding dynamics properties of T70M variant of human lysozyme. *J. Biol. Chem.* **2003**, *278*, 25910−25918.
(95) Johnson, R. J.; Christodoulou, J.; Dumoulin, M.; Caddy, G. L.; Alcocer, M. J.; Murtagh, G. J.; Kumita, J. R.; Larsson, G.; Robinson, C. V.; Archer, D. B. Rationalizing lysozyme amyloidosis: insights from the structure and solution dynamics of T70N lysozyme. *J. Mol. Biol.* **2005**, *352*, 823−836.
(96) Booth, D. R; Sunde, M.; Bellotti, V.; Robinson, C. V.; Hutchinson, W. L.; Fraser, P. E.; Hawkins, P. N.; Dobson, C. M.; Radford, S. E.; Blake, C. C.; Pepys, M. B. Instability, unfolding, and aggregation of human lysozyme variants underlying amyloid fibrillogenesis. *Nature* **1997**, *385*, 787−793.
(97) Canet, D.; Last, A. M.; Tito, P.; Sunde, M.; Spencer, A.; Archer, D. B.; Redfield, C.; Robinson, C. V.; Dobson, C. M. Local cooperativity in the unfolding of an amyloidogenic variant of human lysozyme. *Nat. Struct. Biol.* **2002**, *9*, 308−315.
(98) Dumoulin, M.; Johnson, J. R. K.; Bellotti, V.; Dobson, C. M. In *Protein Misfolding, Aggregation, and Conformational Diseases*; Sipe, J. D., Ed.; VCH Verlag: Weinheim, Germany, 2007; Vol. *II*, pp 635−656.
(99) Gazova, Z.; Bellova, A.; Daxnerova, Z.; Imrich, J.; Kristian, P.; Tomascikova, J.; Bagelova, J.; Fedunova, D.; Antalik, M. Acridine derivatives inhibit lysozyme aggregation. *Eur. Biophys. J.* **2008**, *37*, 1261−1270.
(100) Antosova, A.; Chelli, B.; Bystrenova, E.; Siposova, K.; Valle, F.; Imrich, J.; Vilkova, M.; Kristian, P.; Biscarini, F.; Gazova, Z. Structure−activity relationship of acridine derivatives to amyloid aggregation of lysozyme. *Biochim. Biophys. Acta* **2011**, *1810*, 465−474.
(101) May, B. C. H.; Fafarman, A. T.; Hong, S. B.; Roger, M.; Deady, L. W.; Prusiner, S. B.; Cohen, F. E. Potent inhibition of scrapie prion replication in cultured cells by bis-acridines. *Proc. Natl. Acad. Sci. U.S.A.* **2003**, *100*, 3416−3421.
(102) Chan, P.-H.; Pardon, E.; Menzer, L.; De Genst, E.; Kumita, J. R.; Christodoulou, J.; Saerens, D.; Brans, A.; Bouillenne, F.; Archer, D. B.; Robinson, C. V.; Muyldermans, S.; Matagne, A.; Redfield, C.; Wyns, L.; Dobson, C. M.; Dumoulin, M. Engineering a camelid antibody fragment that binds to the active site of human lysozyme and inhibits its conversion into amyloid fibrils. *Biochemistry* **2008**, *47*, 11041−11054.
(103) Harmsen, M. M.; De Haard, H. J. Properties, production, and applications of camelid single-domain antibody fragments. *Appl. Microbiol. Biotechnol.* **2007**, *77*, 13−22.
(104) Manley, P. N.; Ancsin, J. B.; Kisilevsky, R. Rapid recycling of cholesterol: the joint biologic role of C-reactive protein and serum amyloid A. *Med. Hypotheses* **2006**, *66*, 784−792.
(105) Yamada, T. Serum amyloid A (SAA): a concise review of biology, assay methods and clinical usefulness. *Clin. Chem. Lab. Med.* **1999**, *37*, 381−388.
(106) Tam, S. P.; Flexman, A.; Hulme, J.; Kisilevsky, R. Promoting export of macrophage cholesterol: the physiological role of a major

acute-phase protein, serum amyloid A. *J. Lipid Res.* **2002**, *43*, 1410−1420.
(107) Gabay, C.; Kushner, I. Acute-phase proteins and other systemic responses to inflammation. *N. Engl. J. Med.* **1999**, *340*, 448−454.
(108) Ajiro, J.; Narita, I.; Sato, F.; Saga, D.; Hasegawa, H.; Kuroda, T.; Nakano, M.; Gejyo, F. SAA1 gene polymorphisms and the risk of AA amyloidosis in Japanese patients with rheumatoid arthritis. *Mod. Rheumatol.* **2006**, *16*, 294−299.
(109) Maury, C. P. J.; Aittoniemi, J.; Tiitinen, S.; Laiho, K.; Kaarela, K.; Hurme, M. Variant mannose-binding factor 2 genotype is a risk factor for reactive systemic amyloidosis in rheumatoid arthritis. *J. Intern. Med.* **2007**, *262*, 466−469.
(110) Hasegawa, H.; Nishi, S. I.; Ito, S.; Saeki, T.; Kuroda, T.; Kimura, H.; Watababe, T.; Nakano, M.; Gejyo, F.; Arakawa, M. High prevalence of serum apolipoprotein E4 isoprotein in rheumatoid arthritis patients with amyloidosis. *Arthritis Rheum.* **1996**, *39*, 1728−1732.
(111) Nakamura, T. Amyloid A amyloidosis secondary to rheumatoid arthritis: pathophysiology and treatments. *Clin. Exp. Rheumatol.* **2011**, *29*, 850−857.
(112) Gertz, M. A.; Kyle, R. A. Secondary systemic amyloidosis: response and survival in 64 patients. *Medicine* **1991**, *70*, 246−256.
(113) Obici, L.; Raimondi, S.; Lavatelli, F.; Bellotti, V.; Merlini, G. Susceptibility to AA amyloidosis in rheumatic diseases: a critical overview. *Arthritis Rheum.* **2009**, *61*, 1435−1440.
(114) Wang, Y.; Srinivasan, S.; Ye, Z.; Aguilera, J. J.; Lopez, M. M.; Colon, W. Serum amyloid A 2.2 refolds into a octomeric oligomer that slowly converts to a more stable hexamer. *Biochem. Biophys. Res. Commun.* **2011**, *407*, 725−729.
(115) Gillmore, J. D.; Lovat, L. B.; Persey, M. R.; Pepys, M. B.; Hawkins, P. N. Amyloid load and clinical outcome in AA amyloidosis in relation to circulating concentration of serum amyloid A protein. *Lancet* **2001**, *358*, 24−29.
(116) Lachmann, H. J.; Goodman, J. J.; Gilbertson, J. A.; Gallimore, J. R.; Sabin, C. A.; Gillmore, J. D.; Hawkins, P. N. Natural history and outcome in systemic AA amyloidosis. *N. Engl. J. Med.* **2007**, *356*, 2361−2371.
(117) Pettersson, T.; Konttinen, Y. T.; Maury, C. P. J. Treatment strategies for amyloid A amyloidosis. *Expert Opin. Pharmacother.* **2008**, *9*, 2117−2128.
(118) Dember, L. M.; Hawkins, P. N.; Hazenberg, B. P. C.; Gorevic, P. D.; Merlini, G.; Butrimiene, I.; Livneh, A.; Lesnyak, O.; Puechal, X; Lachmann, J. J.; Obici, L.; Balshaw, R.; Garceau, D.; Hauck, W.; Skinner, M. Eprodisate for the treatment of renal disease in AA amyloidosis. *N. Engl. J. Med.* **2007**, *356*, 2349−2360.
(119) International Randomized, Double-Blind, Placebo-Controlled, Phase 3 Study of the Efficacy and Safety of KIACTA in Preventing Renal Function Decline in Patients With AA Amyloidosis (Clinical Trials.gov Identifier: NCT01215747). http://clinicaltrials.gov/.
(120) Loyd, S.; Mead, S.; Collinge, J. Genetics of Prion Disease. In *Prion Proteins*; Tatzelt, J., Ed.; Springer: Berlin, 2011, *305*; pp 1−23.
(121) Diaz-Espinoza, R.; Soto, C. Generation of prions in vitro and the protein-only hypothesis. *Prion* **2010**, *4*, 1−7.
(122) Moreno-Gonzalez, I.; Soto, C. Misfolded protein aggregates: mechanisms, structures and potential for disease transmission. *Semin.Cell Dev. Biol.* **2011**, *5*, 482−487.
(123) Weissmann, C.; Aguzzi, A. Approaches to therapy of prion diseases. *Annu. Rev. Med.* **2005**, *56*, 321−344.
(124) Tatzelt, J.; Prusiner, S. B.; Welch, W. J. Chemical chaperones interfere with the formation of scrapie prion protein. *EMBO J.* **1996**, *15*, 6363−6373.
(125) Caspi, S.; Halimi, M.; Yanai, A.; Sasson, S. B.; Taraboulos, A.; Gabizon, R. The anti-prion activity of Congo red. Putative mechanism. *J. Biol. Chem.* **1998**, *273*, 3484−3489.
(126) Perrier, V.; Wallace, A. C.; Kaneko, K.; Safar, J.; Prusiner, S. B.; Cohen, F. E. Mimicking dominant negative inhibition of prion replication through structure-based drug design. *Proc. Natl. Acad. Sci. U.S.A.* **2000**, *97*, 6073−6078.
(127) Kaneko, K.; Zulianello, L.; Scott, M.; Cooper, C. M.; Wallace, A. C.; James, T. L.; Cohen, F. E.; Prusiner, S. B. Evidence for protein X binding to a discontinuous epitope on the cellular prion protein during scrapie prion propagation. *Proc. Natl. Acad. Sci. U.S.A.* **1997**, *94*, 10069−10074.
(128) Reddy, T. R.; Mutter, R.; Heal, W.; Guo, K.; Gillet, V. J.; Pratt, S.; Chen, B. Library design, synthesis, and screening: pyridine dicarbonitriles as potential prion disease therapeutics. *J. Med. Chem.* **2006**, *49*, 607−615.
(129) Guo, K; Mutter, R; Heal, W; Reddy, T. R.; Cope, H; Pratt, S; Thompson, M. J.; Chen, B. Synthesis and evaluation of a focused library of pyridine dicarbonitriles against prion disease. *Eur. J. Med. Chem.* **2008**, *43*, 93−106.
(130) Bolognesi, M. L.; Ai Tran, H. N.; Staderini, M.; Monaco, A.; López-Cobeñas, A.; Bongarzone, S.; Biarnés, X.; López-Alvarado, P.; Cabezas, N.; Caramelli, M.; Carloni, P.; Menéndez, J. C.; Legname, G. Discovery of a class of diketopiperazines as antiprion compounds. *ChemMedChem* **2010**, *5*, 1324−1334.
(131) van den Ouweland, A. M.; Knoop, M. T.; Knoers, V. V.; Markslag, P. W.; Rocchi, M.; Warren, S. T.; Ropers, H. H.; Fahrenholz, F.; Monnens, L. A.; van Oost, B. A. Colocalization of the gene for nephrogenic diabetes insipidus (NDI) and the vasopressin type 2 receptor gene (AVPR2) in the Xq28 region. *Genomics* **1992**, *13*, 1350−1352.
(132) Bichet, D. G. Nephrogenic diabetes insipidus. *Am. J. Med.* **1998**, *105*, 431−442.
(133) Fujiwara, T. M.; Bichet, D. G. Molecular biology of hereditary diabetes insipidus. *J. Am. Soc. Nephrol.* **2005**, *16*, 2836−2846.
(134) Robben, J. H.; Knoers, N. V.; Deen, P. M. Cell biological aspects of the vasopressin type-2 receptor and aquaporin 2 water channel in nephrogenic diabetes insipidus. *Am. J. Physiol.: Renal Physiol.* **2006**, *291*, F257−F270.
(135) McKinley, M. J.; Johnson, A. K. The physiological regulation of thirst and fluid intake. *News Physiol. Sci.* **2004**, *19*, 1−6.
(136) Henderson, R.; Baldwin, J. M.; Ceska, T. A.; Zemlin, F.; Beckmann, E.; Downing, K. H. Model for the structure of bacteriorhodopsin based on high-resolution electron cryo-microscopy. *Mol. Biol.* **1990**, *213*, 899−903.
(137) Czaplewski, C.; Kazmierkiewicx, R.; Ciarkowski, J. Molecular modeling of the human vasopressin V2 receptor/agonist complex. *J. Comput.-Aided Mol. Des.* **1998**, *12*, 275−287.
(138) Czaplewski, C.; Kazmierkiewicx, R.; Ciarkowski, J. Molecular modelling of the vasopressin V2 receptor/antagonist interactions. *Acta Biochem. Pol.* **1998**, *45*, 19−26.
(139) Bichet, D. Vasopressin receptor mutations in nephrogenic diabetes insipidus. *Semin. Nephrol.* **2008**, *28*, 245−251.
(140) Conn, P.; Ulloa-Aguirre, A.; Ito, J.; Janovick, J. G protein-coupled receptor trafficking in health and disease: lessons learned to prepare for therapeutic mutant rescue in vivo. *Pharmacol. Rev.* **2007**, *59*, 225−250.
(141) Morello, J.; Salahpour, A.; Petaja-Repo, U.; Laperriere, A.; Lonergan, M.; Arthus, M.; Nabi, I. R.; Bichet, D.; Bouvier, M. Association of calnexin with wild type and mutant AVPR2 that cause nephrogenic diabetes insipidus. *Biochemistry* **2001**, *40*, 6766−6775.
(142) Rosenthal, W. P.; Seibold, A.; Antaramian, A.; Longergan, M.; Arthus, M.; Hendy, G.; Birnbaumer, M.; Bichet, D. Molecular identification of the gene responsible for congenital nephrogenic diabetes insipidus. *Nature* **1992**, *359*, 233−235.
(143) Reeves, W.; Andreoli, T. Nephrogenic Diabetes Insipidus. In *The Metabolic Basis of Inherited Disease*; Scriver, S., Beaudet, A., Sly, W., Valle, D.; McGraw-Hill: New York, 1989; pp 1985−2001.
(144) Spanakis, E.; Milord, E.; Gragnoli, C. AVPR2 variants and mutations in nephrogenic diabetes insipidus: review and missense mutation significance. *J. Cell. Physiol.* **2008**, *217*, 605−617.
(145) Morello, J.; Salahpour, A.; Laperriere, A.; Bernier, V.; Arthus, M.; Lonergan, M.; Petaja-Repo, U.; Angers, S.; Morin, D.; Bichet, D.; Bouvier, M. Pharmacological chaperones rescue cell-surface expression and function of misfolded V2 vasopressin receptor mutants. *J. Clin. Invest.* **2000**, *105*, 887−895.

(146) Bernier, V.; Bichet, D.; Bouvier, M. Pharmacological chaperone action on G-protein coupled receptors. *Curr. Opin. Pharmacol.* **2004**, *4*, 528−533.
(147) Bernier, V.; Lagace, M.; Lonergan, M.; Arthus, M.; Bichet, D.; Bouvier, M. Pharmacological chaperone action on G-protien-coupled recpetors. *Mol. Endocirnol.* **2004**, *18*, 2074−2084.
(148) Bernier, V.; Morello, J.; Zarruk, A.; Debrand, N.; Salahpour, A.; Lonergan, M.; Arthus, M.; Laperriere, A.; Brouard, R.; Bouvier, M.; Bichet, D. Pharmacologic chaperones as a potential treatment for X-linked nephrogenic diabetes insipidus. *J. Am. Soc. Nephrol.* **2006**, *17*, 232−243.
(149) Cheong, H.; Cho, H.; Park, H.; Ha, I. S.; Choi, Y. Molecular genetic study of congenital nephrogenic diabetes insipidus and rescue of mutant vasopressin V2 receptor by chemical chaperones. *Nephrology* **2007**, *12*, 113−117.
(150) Robben, J.; Sze, M.; Knoers, N.; Deen, P. Rescue of vasopressin V2 receptor mutants by chemical chaperones: specificity and mechanism. *Mol. Biol. Cell* **2006**, *17*, 379−386.
(151) Wuller, S.; Wiesner, B.; Loffler, A.; Furkert, J.; Krause, G.; Hermosilla, R.; Schaefer, M.; Schulein, R.; Rosenthal, W.; Oksche, A. Pharmacochaperones post-translationally enhance cell surface expression by increasing conformational stability of wild-type and mutant vasopressin V2 receptors. *J. Biol. Chem.* **2004**, *279*, 47254−47263.
(152) Oueslati, M.; Hermosilla, R.; Schonenberger, E.; Oorschot, V.; Beyermann, M.; Wiesner, B.; Schmidt, A.; Klumperman, J.; Rosenthal, W.; Schulein, R. Rescue of a nephrogenic diabetes insipidus-causing vasopressin V2 receptor mutant by cell-penetrating peptides. *J. Biol. Chem.* **2007**, *282*, 20676−20685.
(153) Valenzano, K. J.; Benjamin, E. R.; Rene, P.; Bouvier, M. Pharmacological Chaperones: Potential for the Treatment of Hereditary Diseases Caused by Mutations in G Protein-Coupled Receptors. In *GPCR Molecular Pharmacology and Drug Targeting: Shifting Paradigms and New Direction*; Gilchrist, A., Ed.; John Wiley & Sons, Inc.: Hoboken, NJ, 2010,
(154) Robben, J.; Deen, P. Pharmacological chaperones in nephrogenic diabetes insipidus. *BioDrugs* **2007**, *21*, 157−166.
(155) Stockley, R. A. Emerging drugs for alpha-1-antitrypsin deficiency. *Expert Opin. Emerging Drugs* **2010**, *15*, 685−694.
(156) Perlmutter, D. H. Liver injury in alpha-1-antitrypsin deficiency: an aggregated protein induces mitochondrial injury. *J. Clin. Invest.* **2002**, *110*, 1579−1583.
(157) Greene, C. M.; McElvaney, N. G. Protein misfolding and obstructive lung disease. *Proc. Am. Thorac. Soc.* **2010**, *7*, 346−355.
(158) Dafforn, T. R.; Mahadeva, R.; Elliott, P. R.; Sivasothy, P.; Lomas, D. A. A kinetic mechanism for the polymerisation of alpha-1-antitrypsin. *J. Biol. Chem.* **1999**, *274*, 9548−9555.
(159) Purkayastha, P.; Klemke, J. W.; Lavender, S.; Oyola, R.; Cooperman, B. S.; Gai, F. alpha-1-Antitrypsin polymerisation: a fluorescence correlation spectroscopic study. *Biochemistry* **2005**, *44*, 2642−2649.
(160) Huntington, J. A.; Read, R. J.; Carrell, R. W. Structure of a serpin-protease complex shows inhibition by deformation. *Nature* **2000**, *407*, 923−926.
(161) *Molecular Operating Environment (MOE)*, version 2011.10; Chemical Computing Group Inc. (1010 Sherbooke St. West, Suite No. 910, Montreal, Quebec, Canada, H3A 2R7), 2011.
(162) Stoller, J. K.; Aboussouan, L. S. alpha-1-Antitrypsin deficiency. *Lancet* **2005**, *365*, 2225−2236.
(163) http://clinicaltrials.gov/ct2/show/NCT00670007?term=alpha-1-antitrypsin&phase=3&rank=2.
(164) Bathurst, I. C.; Travis, J.; George, P. M.; Carrell, R. W. Structural and functional characterization of the abnormal Z alpha-1-antitrypsin isolated from human liver. *FEBS Lett.* **1984**, *177*, 179−183.
(165) Ogushi, F.; Fells, G. A.; Hubbard, R. C.; Straus, S. D.; Crystal, R. G. Z-Type alpha-1-antitrypsin is less competent than M1-type alpha-1-antitrypsin as an inhibitor of neutrophil elastase. *J. Clin. Invest.* **1987**, *80*, 1366−1374.
(166) Burrows, J. A.; Willis, L. K.; Perlmutter, D. H. Chemical chaperones mediate increased secretion of mutant alpha-1-antitrypsin Z: a potential pharmacological strategy for prevention of liver injury and emphysema in alpha-1-antitrypsin deficiency. *Proc. Natl. Acad. Sci. U.S.A.* **2000**, *97*, 1796−1801.
(167) Sharpe, L. K.; Mallya, M.; Kinghorn, K. J.; Wang, Z.; Crowther, D. C.; Huntington, J. A.; Belorgey, D.; Lomas, D. A. Sugar and alcohol molecules provide a therapeutic strategy for the serpinopathies that cause dementia and cirrhosis. *FEBS J.* **2006**, *273*, 2540−2552.
(168) Zhou, A.; Stein, P. E.; Huntington, J. A.; Carrell, R. W. Serpin polymerisation is prevented by a hydrogen-bond network which is centered on His 334 and stabilised by glycerol. *J. Biol. Chem.* **2003**, *278*, 15116−15122.
(169) Teckman, J. H. Lack of effect of oral 4-phenylbutyrate on serum alpha-1-antitrypsin in patients with alpha-1-antitrypsin deficiency: a preliminary study. *J. Pediatr. Gastroenterol. Nutr.* **2004**, *1* (39), 34−37.
(170) Mallya, M.; Phillips, R. L.; Saldanha, S. A.; Gooptu, B.; Brown, S. C. L.; Termine, D. J.; Shirvani, A. M.; Wu, Y.; Sifers, R. N.; Abagyan, R.; Lomas, D. A. Small molecules block the polymerization of Z alpha-1-antitrypsin and increase the clearance of intracellular aggreagates. *J. Med. Chem.* **2007**, *50*, 5357−5363.
(171) Lee, C.; Maeng, J. S.; Kocher, J. P.; Lee, B.; Yu, M. H. Cavities of alpha-1-antitrypsin that play structural and functional roles. *Protein Sci.* **2001**, *10*, 1446−1453.
(172) Parfrey, H; Mahadeva, R.; Ravenhill, N.; Zhou, A.; Dafforn, T. R. Targeting a surface cavity of alpha-1-antitrypsin to prevent conformational disease. *J. Biol. Chem.* **2003**, *278*, 33060−33066.
(173) Chang, Y.-P.; Mahadeva, R.; Chang, W.-S. W.; Lin, S.-C.; Chu, Y.-H. Small molecule peptides inhibit Z alpha1-antitrypsin polymerization. *J. Cell. Mol. Med.* **2009**, *13*, 2304−2316.
(174) Schulze, A. J.; Baumann, U.; Knof, S.; Jaeger, E.; Huber, R.; Laurell, C. B. Structural transition of alpha1-antitrypsin by a peptide sequentially similar to beta-strand s4A. *Eur. J. Biochem.* **1990**, *194*, 51−56.